Modeling the Transport of Suspended Particles Using LES

Accounting for Finite-Size Effects in a Continuum Model

ATELIER TURBULENCE DE L'OSUG | 2ÈME JOURNÉE

DECEMBER 5, 2024

Julien CHAUCHAT

Associate Professor
University Grenoble Alpes
LEGI, Grenoble, France
Industrial chair of excellence OXALIA

→

Senior Researcher @ INRAE
University Grenoble Alpes
IGE, Grenoble, France

Université Grenoble Alpes | Grenoble INP UGA | LEGI | oxalia BY FONDATION GRENOBLE INP | cnrs

HUNTER ROUSE EXPERIMENTS (ICTAM 1938)

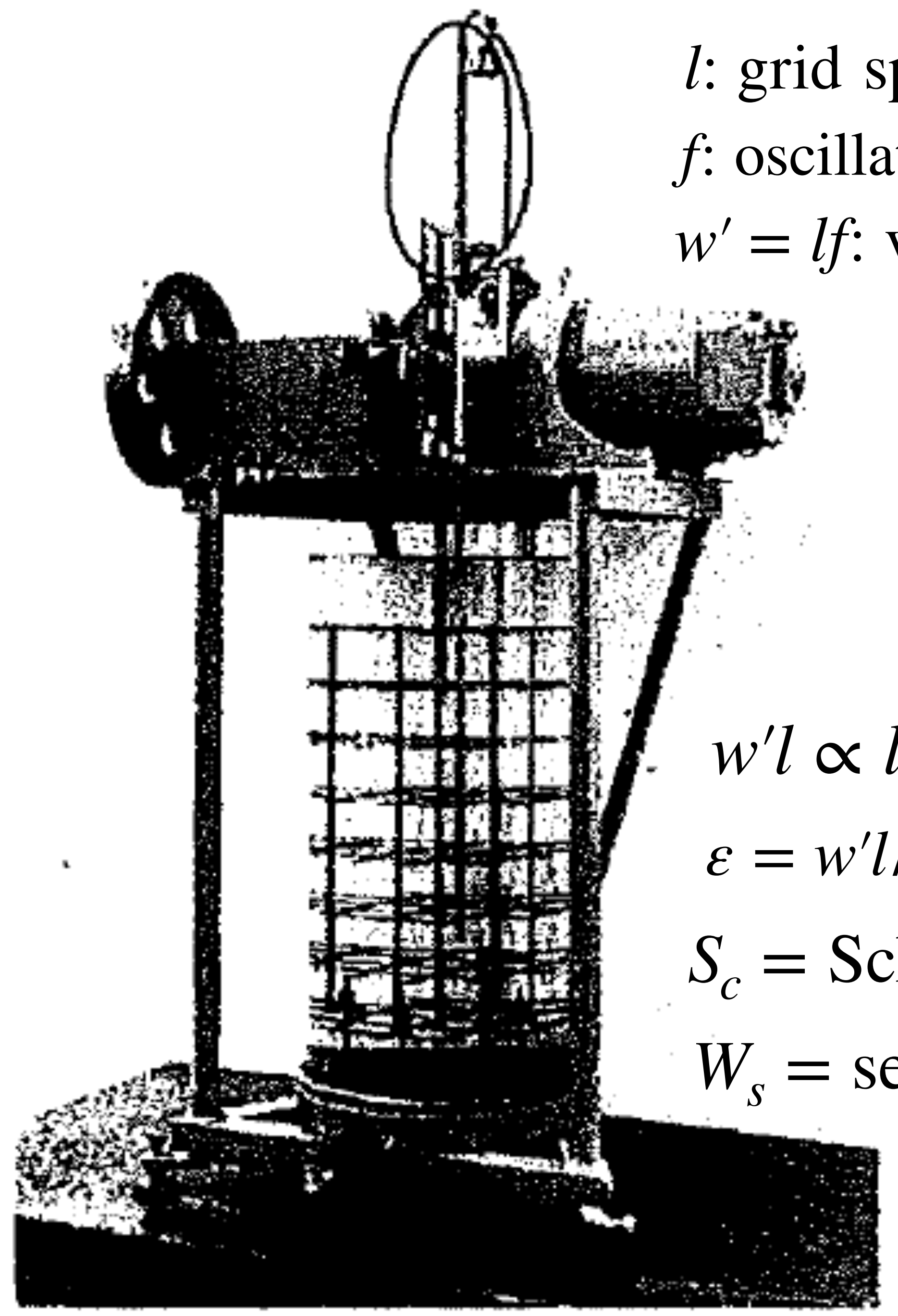

l: grid spacing (m)

f: oscillation freq. (Hz)

$w' = lf$: vel. fluc. (m/s)

$w'l \propto l^2 f = \text{cst}$

$\varepsilon = w'l/S_c$

S_c = Schmidt number

W_s = settling velocity

Fig.1 General view of experimental apparatus.

Nominal diameter d	Size range	Sieve mesh	Settling velocity	Reynolds number
1/4 mm	.351 -- .246 mm	42 -- 50	3.69 cm/s	11.0
1/8 mm	.175 -- .124 mm	80 -- 115	1.75 cm/s	2.6
1/16 mm	.088 -- .061 mm	170 -- 250	0.675 cm/s	0.5
1/32 mm	.053 -- .037 mm	----	0.131 cm/s	0.06

HUNTER ROUSE EXPERIMENTS (ICTAM 1938)

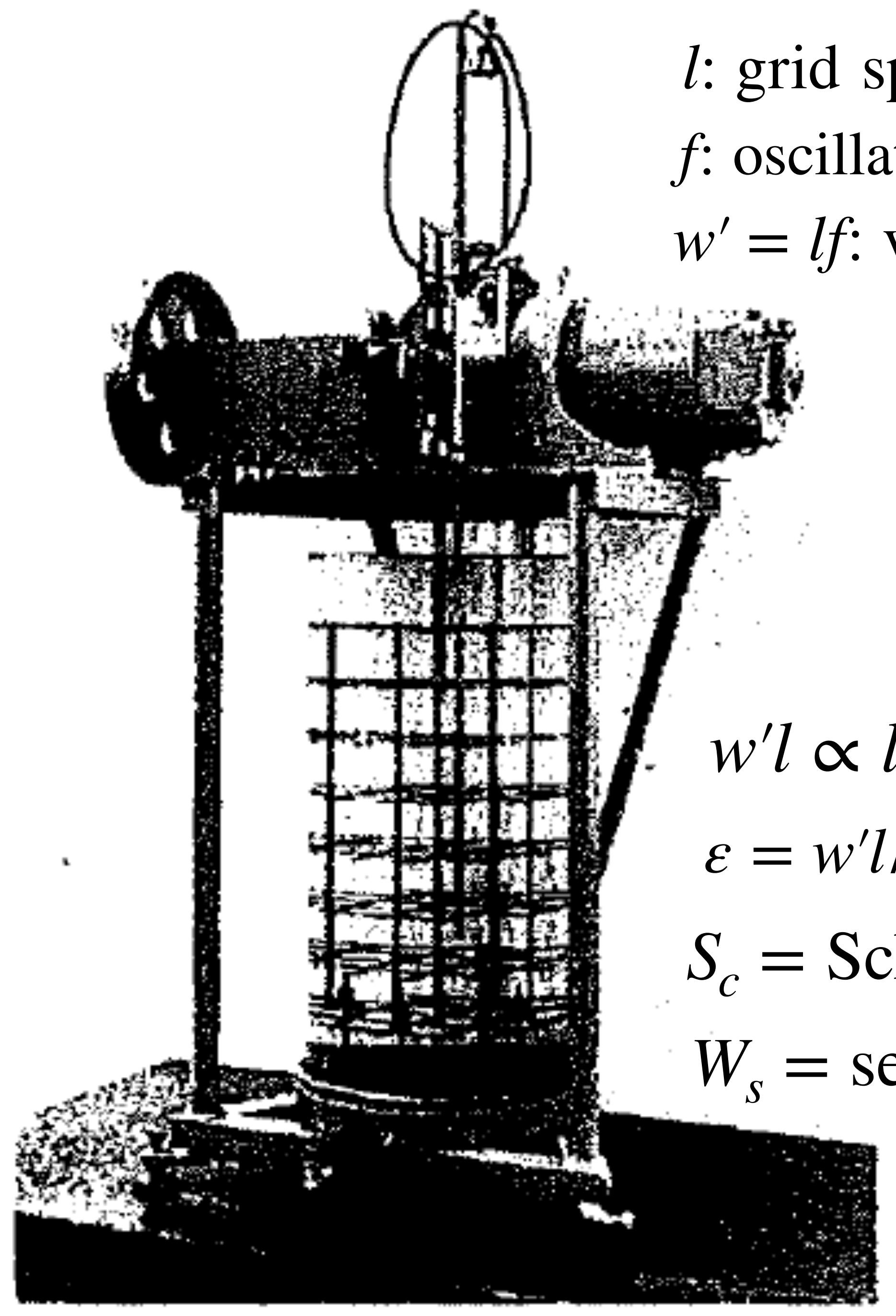

l: grid spacing (m)

f: oscillation freq. (Hz)

$w' = lf$: vel. fluc. (m/s)

$w'l \propto l^2 f = \text{cst}$

$\varepsilon = w'l/S_c$

S_c = Schmidt number

W_s = settling velocity

Fig.1 General view of experimental apparatus.

Nominal diameter d	Size range	Sieve mesh	Settling velocity	Reynolds number
1/4 mm	.351 -- .246 mm	42 -- 60	3.69 cm/s	11.0
1/8 mm	.175 -- .124 mm	80 -- 115	1.75 cm/s	2.6
1/16 mm	.088 -- .061 mm	170 -- 250	0.675 cm/s	0.5
1/32 mm	.053 -- .037 mm	----	0.131 cm/s	0.06

Reynolds-averaged Mass balance: $-W_s c + \overline{w'c'} = 0$

HUNTER ROUSE EXPERIMENTS (ICTAM 1938)

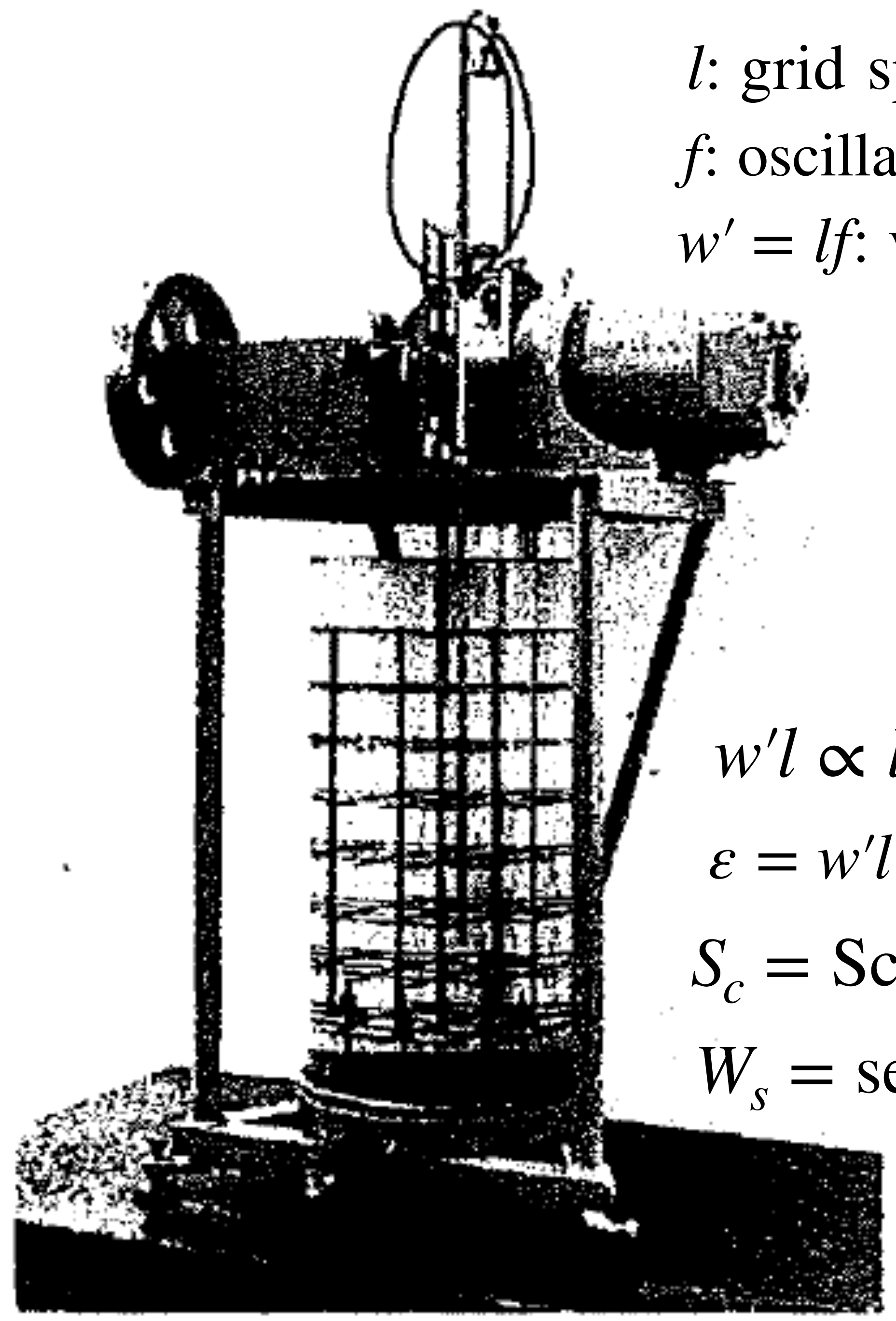

l: grid spacing (m)

f: oscillation freq. (Hz)

$w' = lf$: vel. fluc. (m/s)

$w'l \propto l^2 f = \text{cst}$

$\varepsilon = w'l / S_c$

S_c = Schmidt number

W_s = settling velocity

Fig.1 General view of experimental apparatus.

Nominal diameter d	Size range	Sieve mesh	Settling velocity	Reynolds number
1/4 mm	.351 -- .246 mm	42 -- 50	3.69 cm/s	11.0
1/8 mm	.175 -- .124 mm	80 -- 115	1.75 cm/s	2.6
1/16 mm	.088 -- .061 mm	170 -- 250	0.675 cm/s	0.5
1/32 mm	.053 -- .037 mm	----	0.131 cm/s	0.06

Reynolds-averaged Mass balance: $-W_s c + \overline{w'c'} = 0$

Net rate of turbulent transport: $\overline{w'c'} = -\varepsilon_s \dfrac{dc}{dy}$

HUNTER ROUSE EXPERIMENTS (ICTAM 1938)

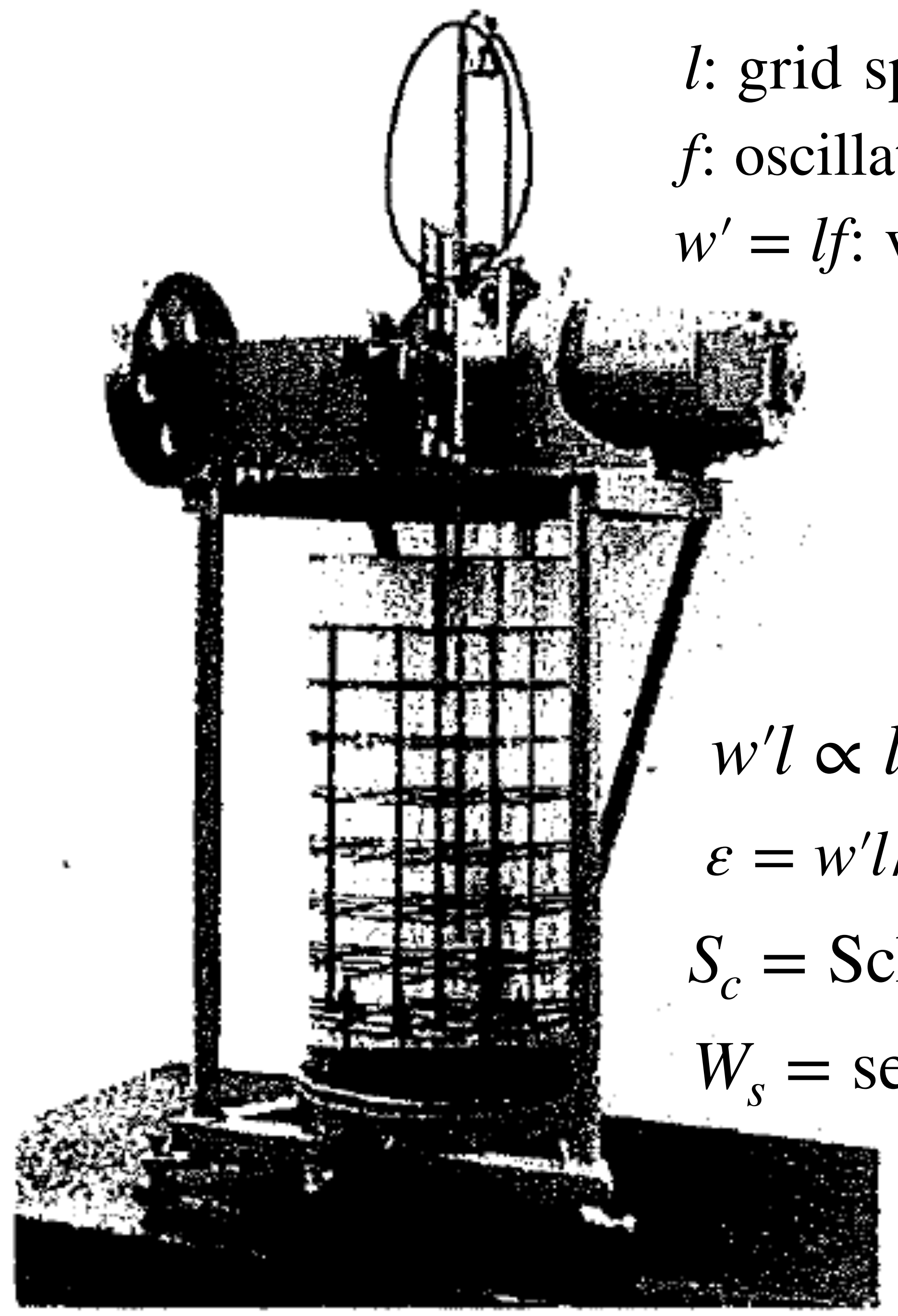

l: grid spacing (m)
f: oscillation freq. (Hz)
$w' = lf$: vel. fluc. (m/s)

$w'l \propto l^2 f = \text{cst}$
$\varepsilon = w'l / S_c$
S_c = Schmidt number
W_s = settling velocity

Fig.1 General view of experimental apparatus.

Nominal diameter d	Size range	Sieve mesh	Settling velocity	Reynolds number
1/4 mm	.351 -- .246 mm	42 -- 60	3.69 cm/s	11.0
1/8 mm	.175 -- .124 mm	80 -- 115	1.75 cm/s	2.6
1/16 mm	.088 -- .061 mm	170 -- 250	0.675 cm/s	0.5
1/32 mm	.053 -- .037 mm	----	0.131 cm/s	0.06

Reynolds-averaged Mass balance: $-W_s c + \overline{w'c'} = 0$

Net rate of turbulent transport: $\overline{w'c'} = -\varepsilon_s \dfrac{\mathrm{d}c}{\mathrm{d}y}$

Concentration profile: $\dfrac{c(y)}{c_a} = e^{-W_s/\varepsilon_s (y-a)} \Rightarrow \log\left(c(y)/c_a\right) \propto y - a$

HUNTER ROUSE EXPERIMENTS (ICTAM 1938)

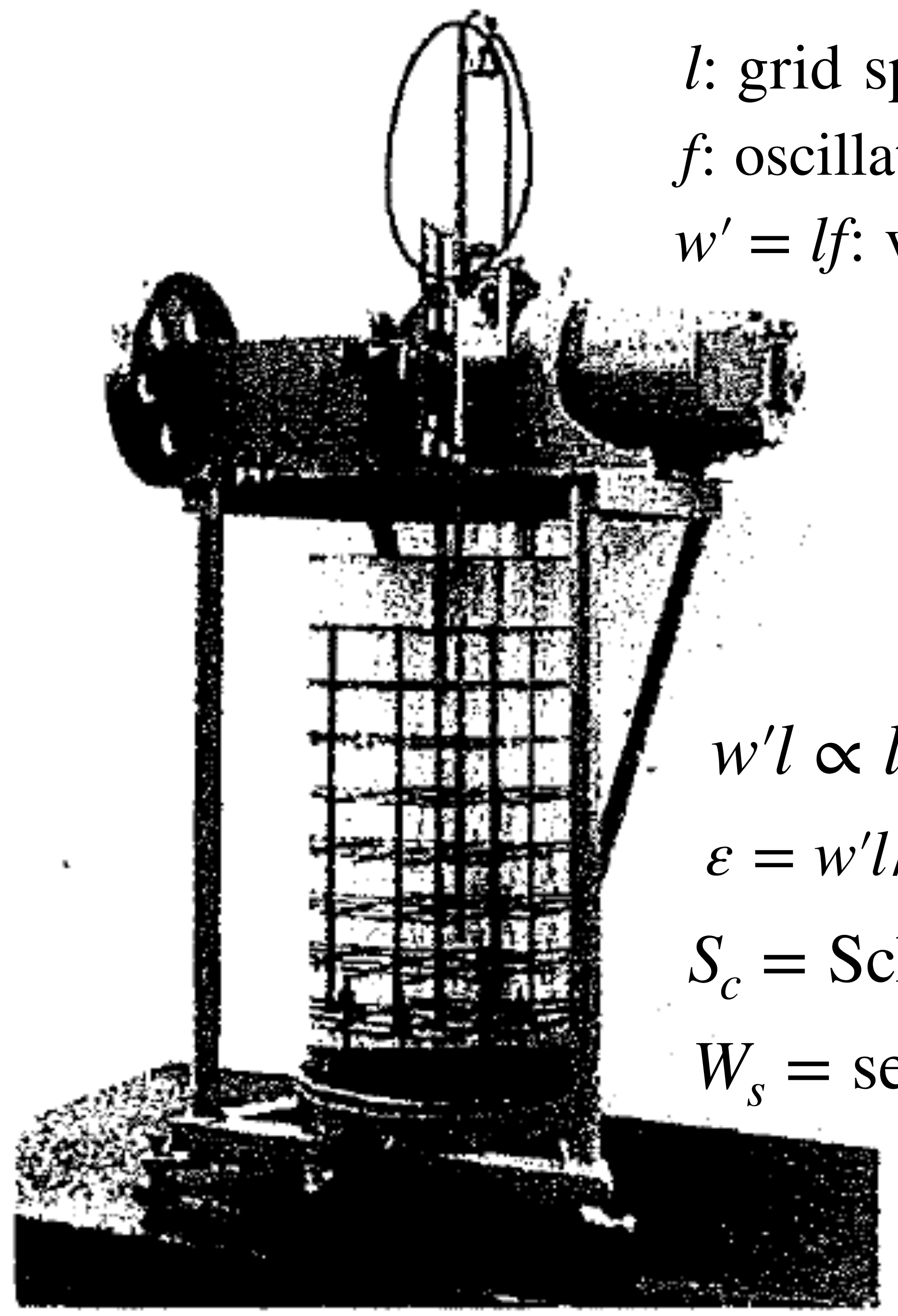

l: grid spacing (m)

f: oscillation freq. (Hz)

$w' = lf$: vel. fluc. (m/s)

$w'l \propto l^2 f = \text{cst}$

$\varepsilon = w'l/S_c$

S_c = Schmidt number

W_s = settling velocity

Fig.1 General view of experimental apparatus.

Nominal diameter d	Size range	Sieve mesh	Settling velocity	Reynolds number
1/4 mm	.351 -- .246 mm	42 -- 60	3.69 cm/s	11.0
1/8 mm	.175 -- .124 mm	80 -- 115	1.75 cm/s	2.6
1/16 mm	.088 -- .061 mm	170 -- 250	0.675 cm/s	0.5
1/32 mm	.053 -- .037 mm	----	0.131 cm/s	0.06

Reynolds-averaged Mass balance: $-W_s c + \overline{w'c'} = 0$

Net rate of turbulent transport: $\overline{w'c'} = -\varepsilon_s \dfrac{dc}{dy}$

Concentration profile: $\dfrac{c(y)}{c_a} = e^{-W_s/\varepsilon_s (y-a)} \Rightarrow \log\left(c(y)/c_a\right) \propto y - a$

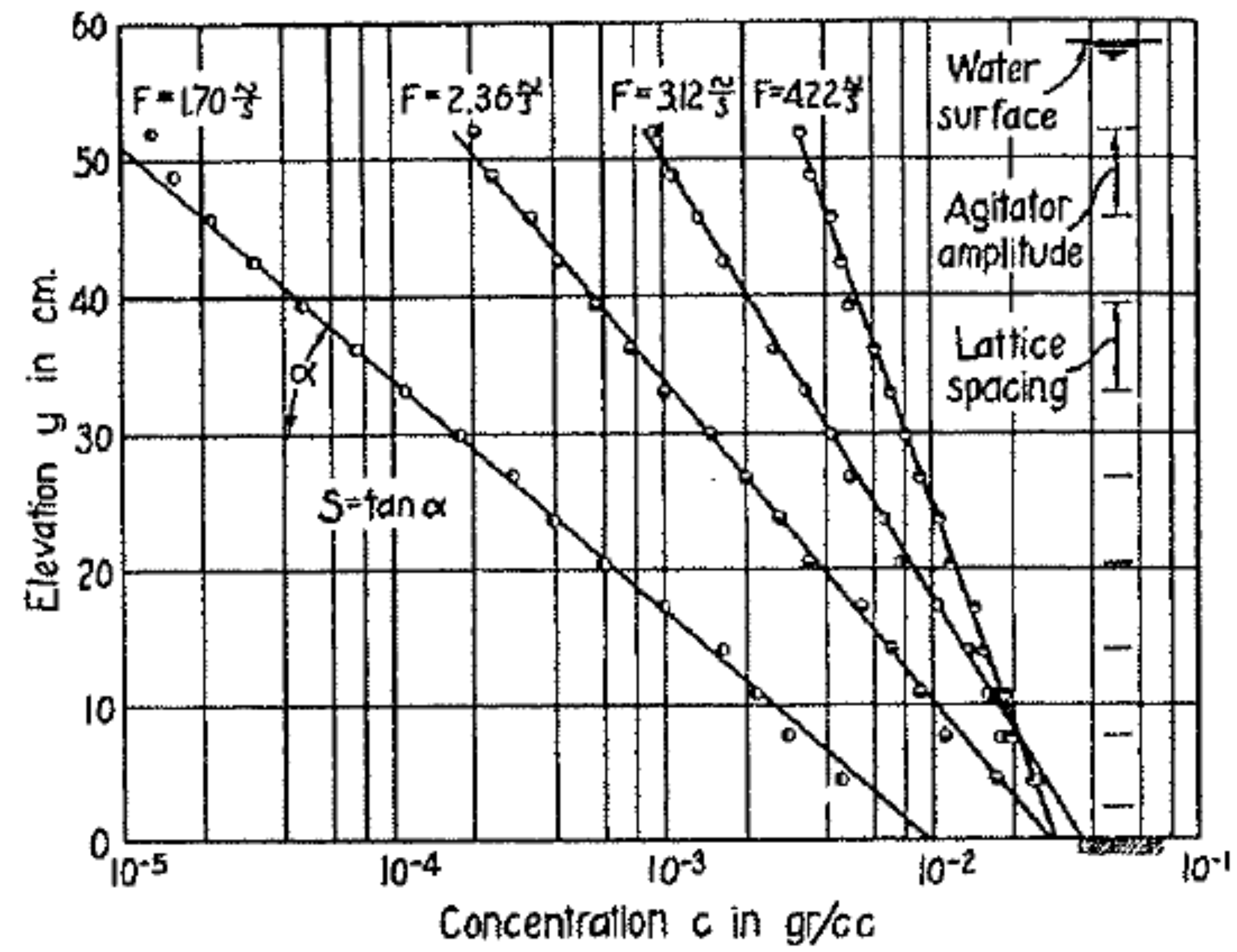

OPEN-CHANNEL FLOWS

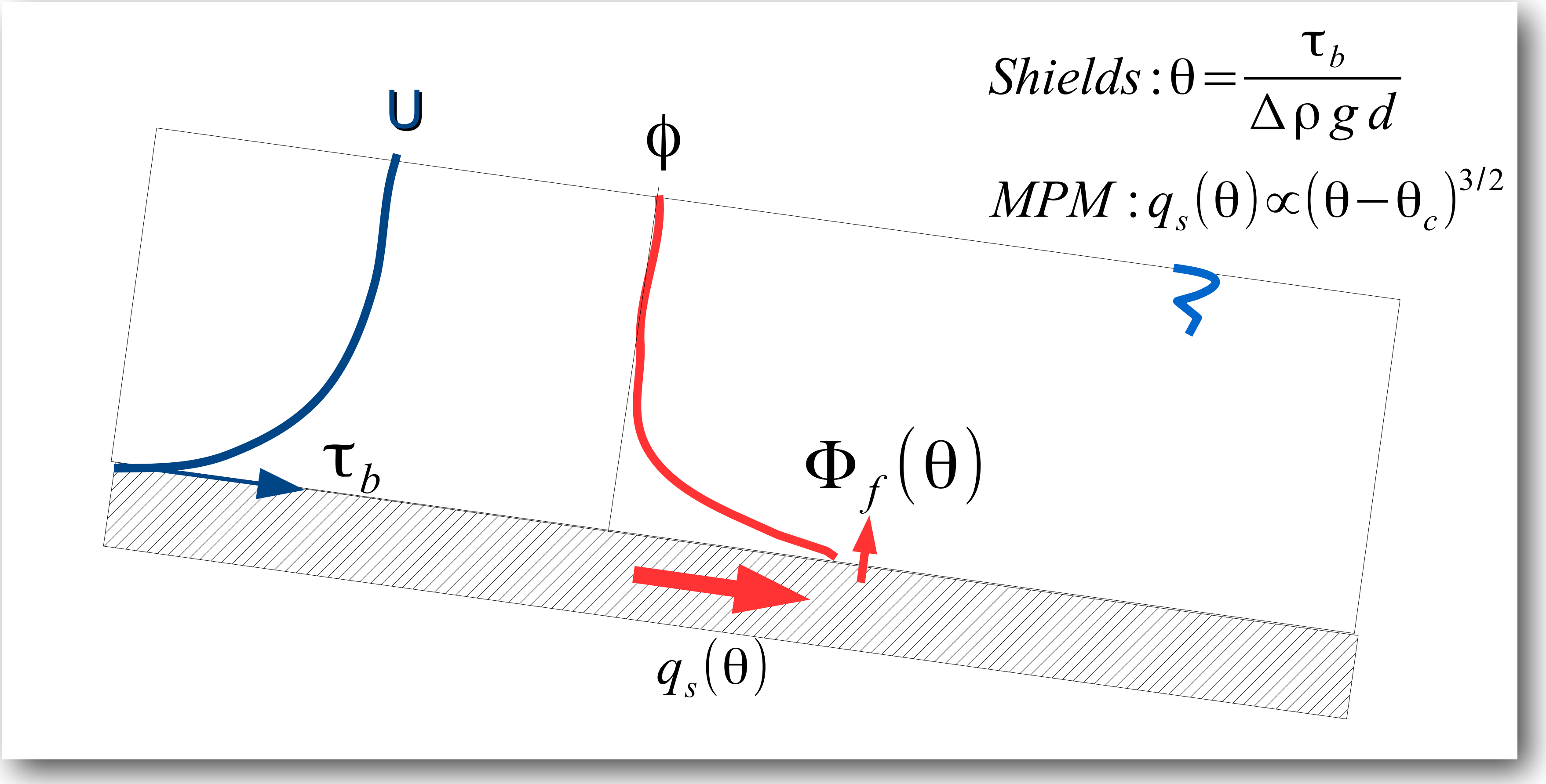

Eddy viscosity: $\nu^t = \kappa\ u_*\ z\ (1 - z/H_f)$

Concentration diffusivity: $\varepsilon_s = \dfrac{\nu^t}{S_c}$

Rouse profile: $\dfrac{c}{c_a} = \left[\dfrac{z}{H_f - z}\dfrac{H_f - a}{a}\right]^{-Ro}$

Rouse number: $Ro = \dfrac{S_c W_s}{\kappa u_*}$

OPEN-CHANNEL FLOWS

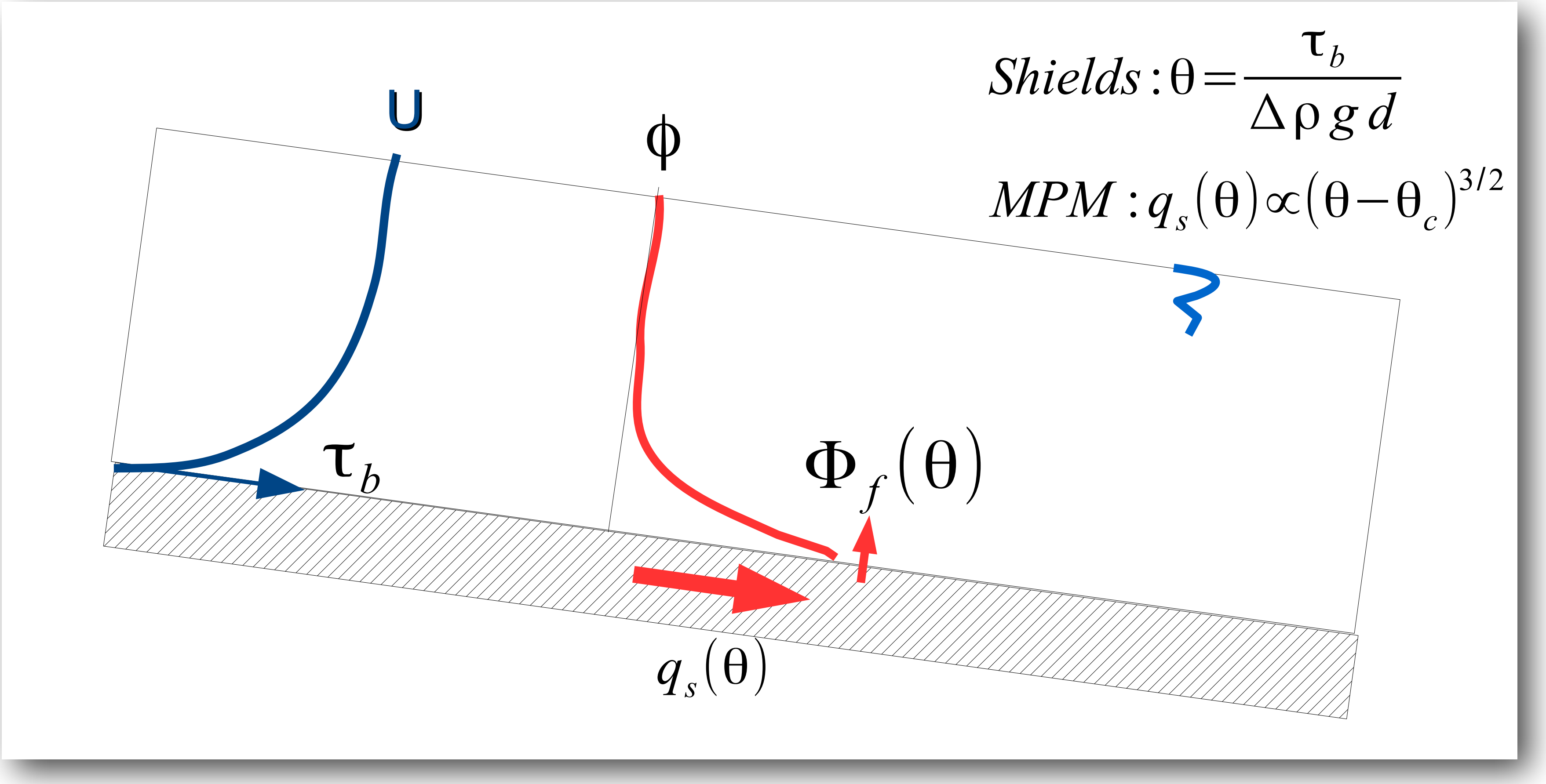

Eddy viscosity: $\nu^t = \kappa \; u_* \; z \; (1 - z/H_f)$

Concentration diffusivity: $\varepsilon_s = \dfrac{\nu^t}{S_c}$

Rouse profile: $\dfrac{c}{c_a} = \left[\dfrac{z}{H_f - z} \dfrac{H_f - a}{a} \right]^{-Ro}$

Rouse number: $Ro = \dfrac{S_c W_s}{\kappa u_*}$

Turbulent Schmidt number: S_c

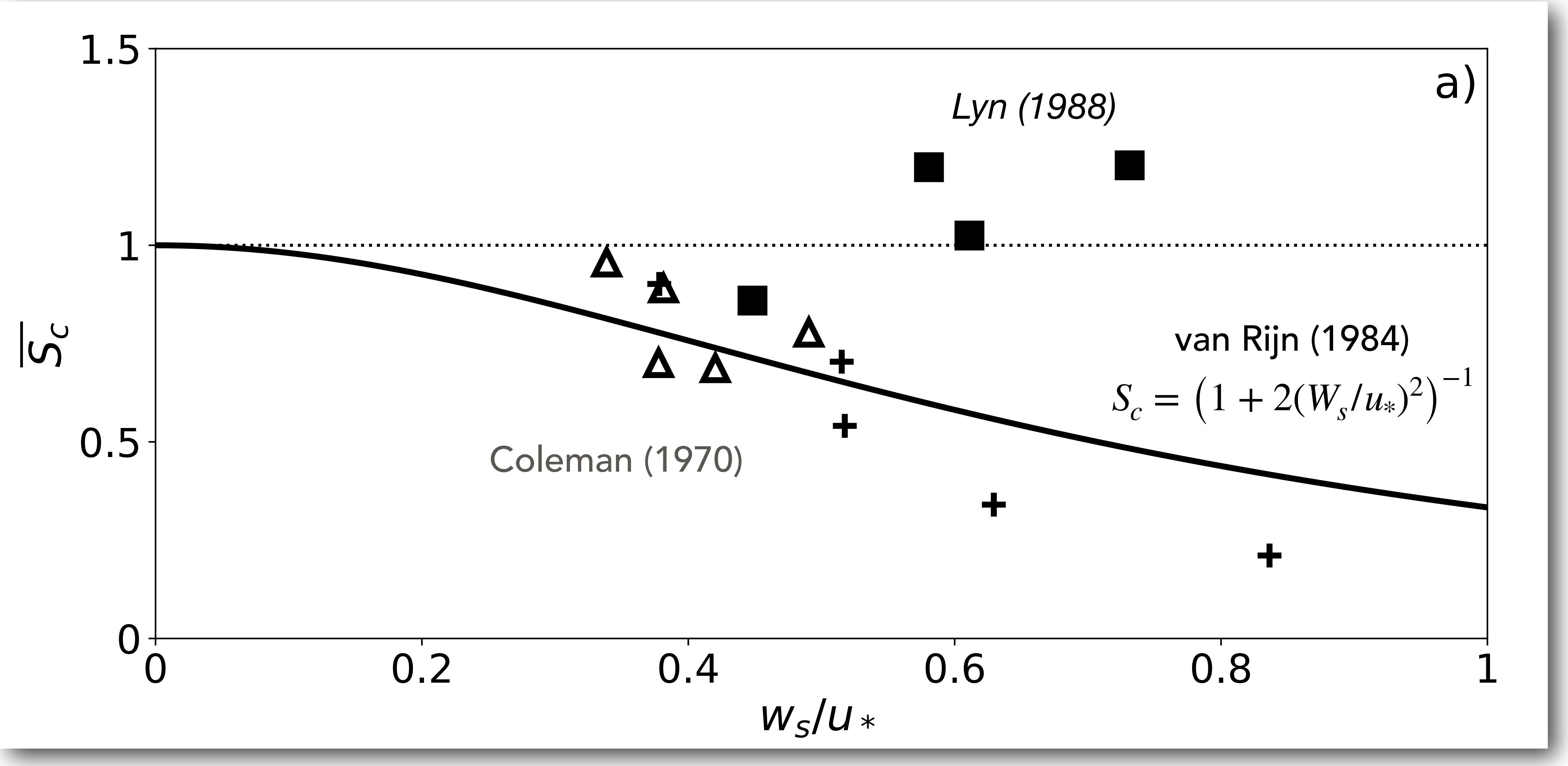

Data from open-channel flow experiments collected by Lyn (2008)

OPEN-CHANNEL FLOWS

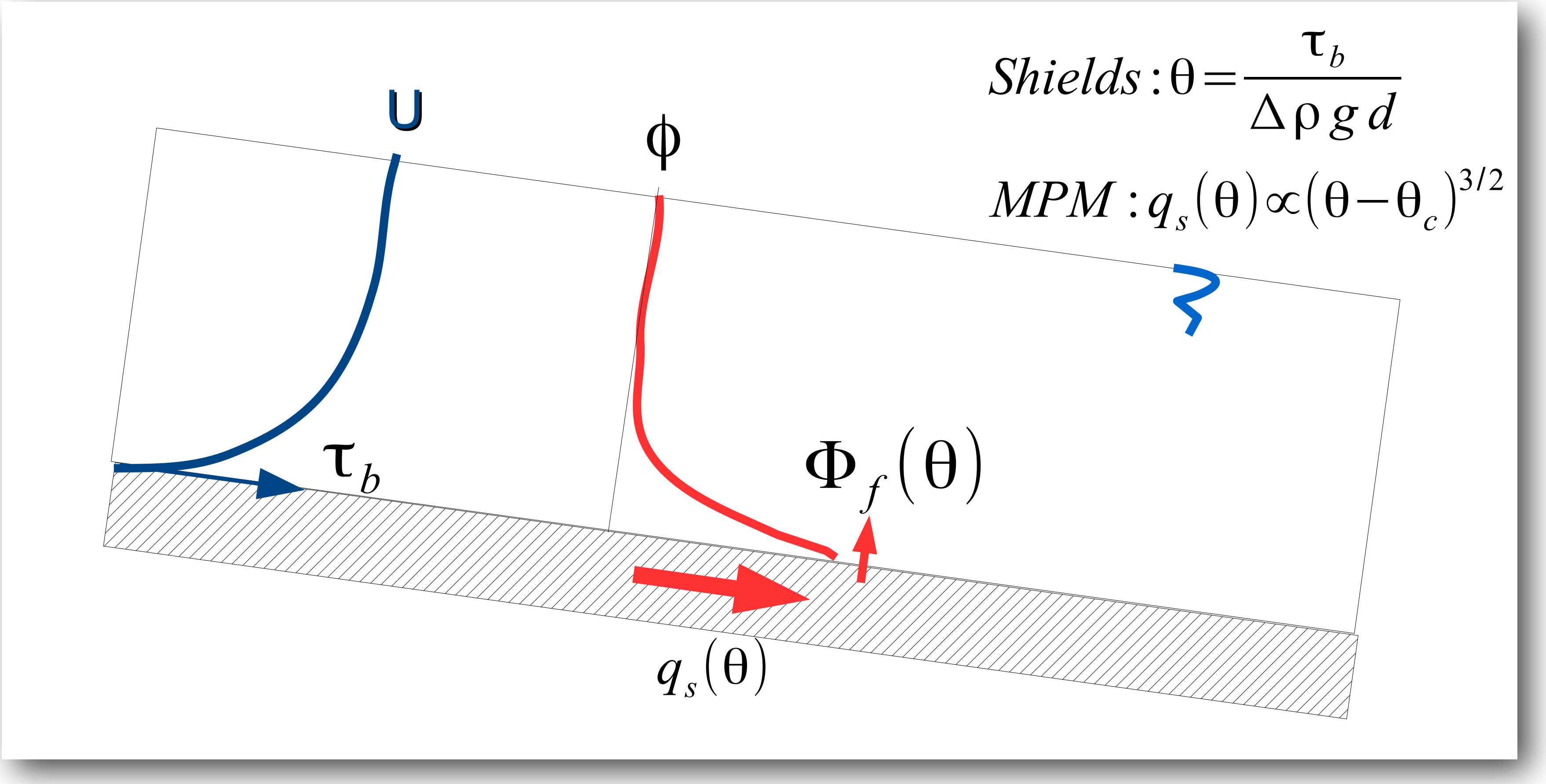

Eddy viscosity: $\nu^t = \kappa\ u_*\ z\ (1 - z/H_f)$

Concentration diffusivity: $\varepsilon_s = \dfrac{\nu^t}{S_c}$

Rouse profile: $\dfrac{c}{c_a} = \left[\dfrac{z}{H_f - z}\dfrac{H_f - a}{a}\right]^{-Ro}$

Rouse number: $Ro = \dfrac{S_c W_s}{\kappa u_*}$

Turbulent Schmidt number: S_c

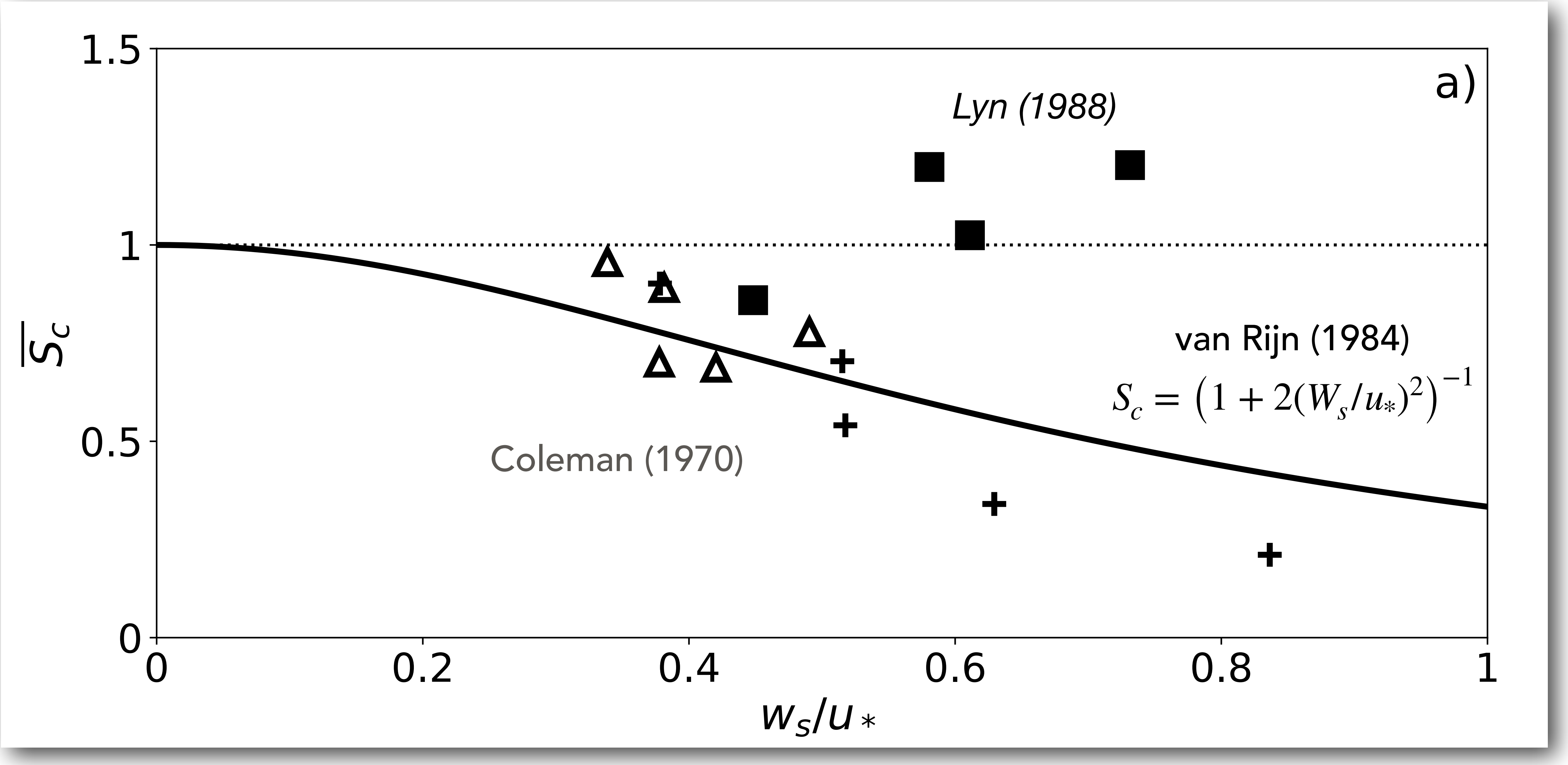

Data from open-channel flow experiments collected by Lyn (2008)

What could explain $S_c < 1$?

Eulerian-Eulerian two-phase flow equations

Local mass & momentum conservation for a fluid-particle mixture

$$\nabla.\vec{u} = 0 \quad \text{and} \quad \frac{d\rho\vec{u}}{dt} + \nabla.(\rho\vec{u} \otimes \vec{u}) = \nabla.\overline{\overline{\sigma}} + \rho\vec{g}$$

Local spatial averaging

Jackson (2000)

Eulerian-Eulerian two-phase flow equations

Local mass & momentum conservation for a fluid-particle mixture

$$\nabla.\vec{u} = 0 \quad \text{and} \quad \frac{d\rho\vec{u}}{dt} + \nabla.(\rho\vec{u}\otimes\vec{u}) = \nabla.\overline{\overline{\sigma}} + \rho\vec{g}$$

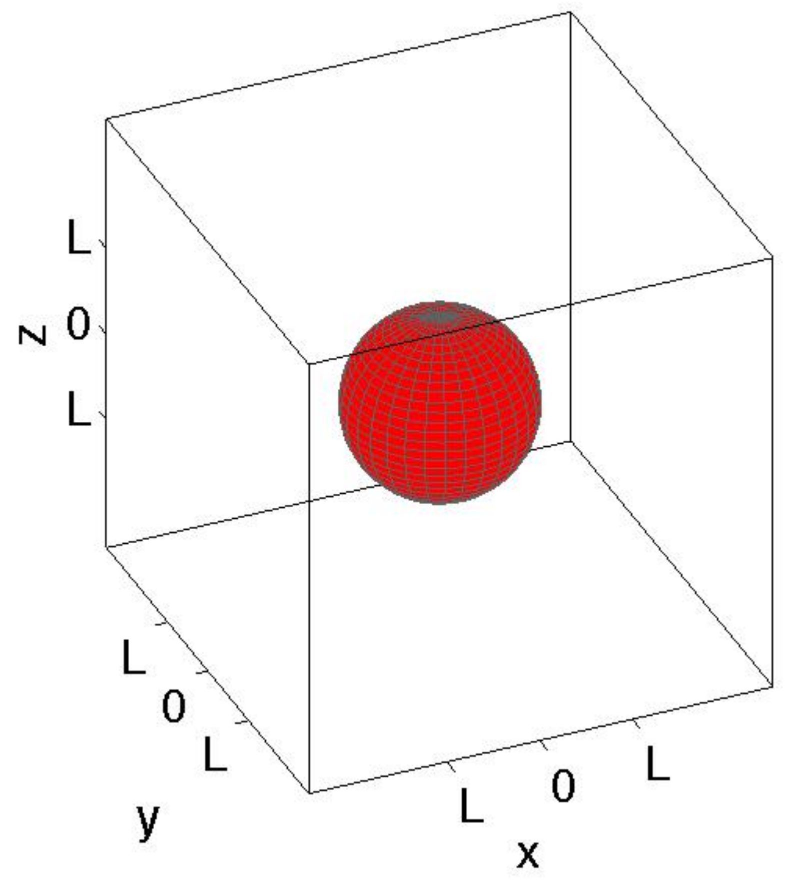

G_L is a 3D door function

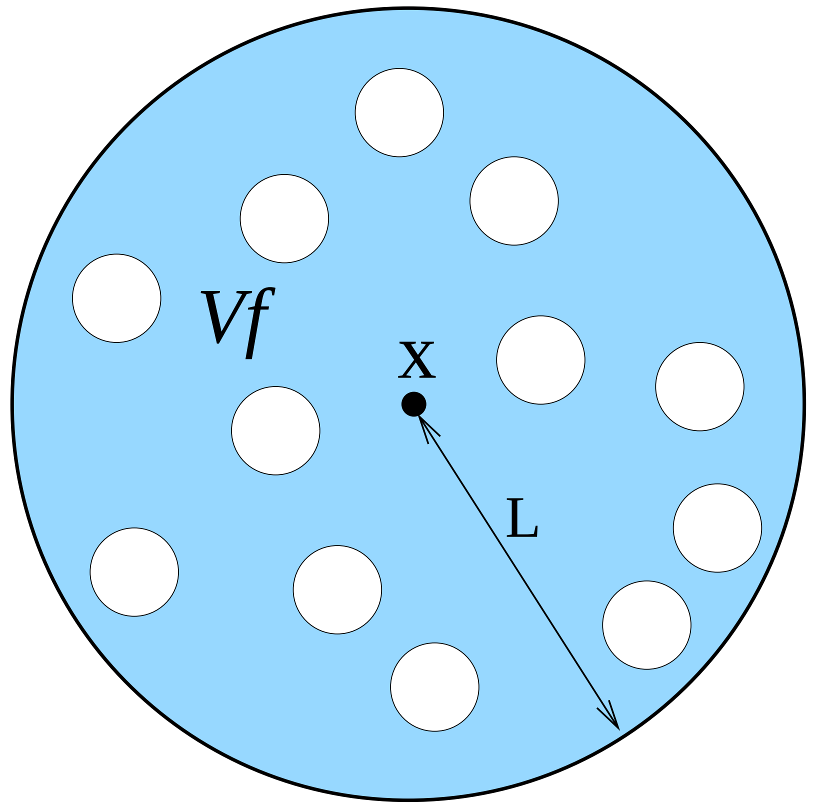

Local spatial averaging

Jackson (2000)

$$L_{flow} >> L >> d$$

$$\langle f\rangle^f(\vec{x},t) = \frac{1}{1-\phi(\vec{x},t)}\int_{V_f(t)} f(\vec{y},t)G_L(|\vec{x}-\vec{y}|)dV_y$$

Eulerian-Eulerian two-phase flow equations

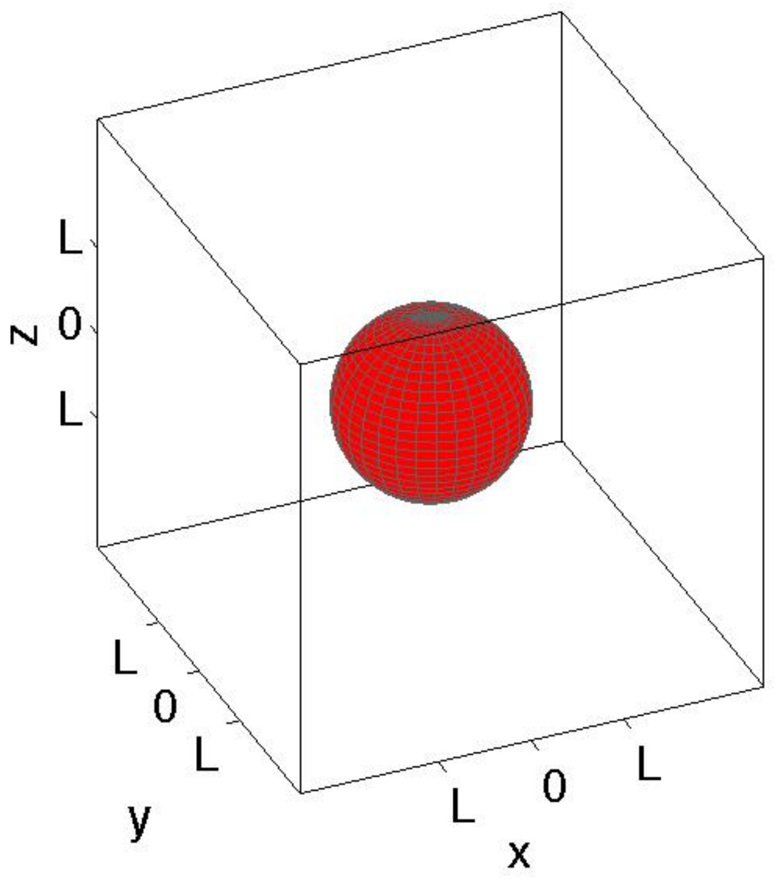

G_L is a 3D door function

Local mass & momentum conservation for a fluid-particle mixture

$$\nabla.\vec{u} = 0 \quad \text{and} \quad \frac{d\rho\vec{u}}{dt} + \nabla.(\rho\vec{u} \otimes \vec{u}) = \nabla.\overline{\overline{\sigma}} + \rho\vec{g}$$

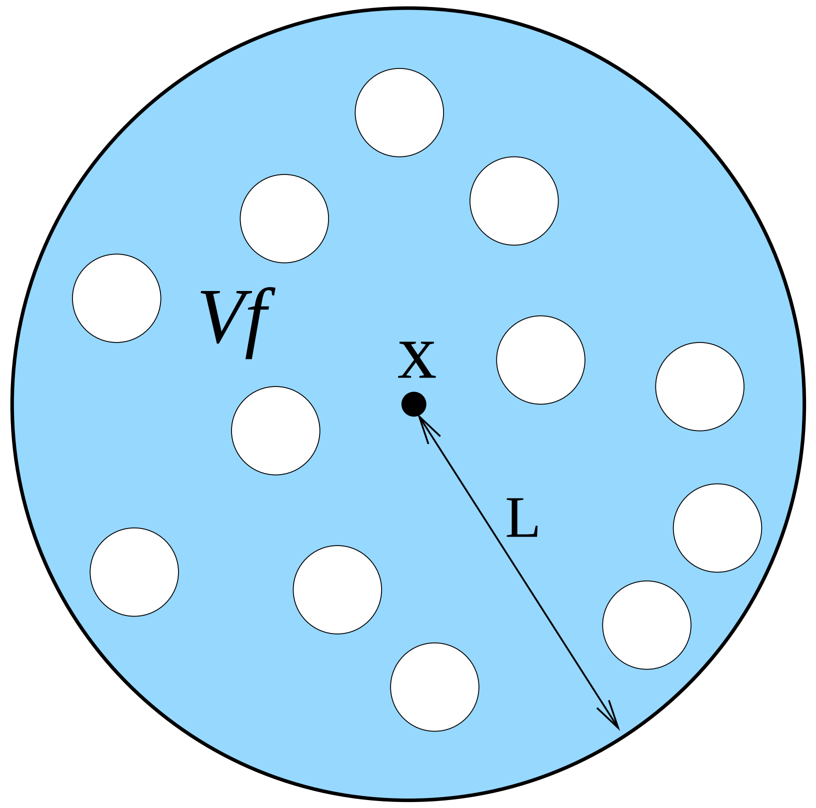

Local spatial averaging

Jackson (2000)

$$L_{flow} >> L >> d$$

$$\langle f \rangle^f(\vec{x}, t) = \frac{1}{1 - \phi(\vec{x}, t)} \int_{V_f(t)} f(\vec{y}, t) G_L(|\vec{x} - \vec{y}|) dV_y$$

Fluid phase mass and momentum equations

$$\frac{\partial(1-\phi)}{\partial t} + \nabla \cdot \left((1-\phi)\langle\vec{u}\rangle^f\right) = 0$$

$$\rho^f \left[\frac{\partial(1-\phi)\langle\vec{u}\rangle^f}{\partial t} + \nabla\left((1-\phi)\langle\vec{u}\rangle^f \otimes \langle\vec{u}\rangle^f\right)\right] = \nabla\overline{\overline{\sigma^f}} - n\vec{f} + (1-\phi)\rho^f g$$

Eulerian-Eulerian two-phase flow equations

Local mass & momentum conservation for a fluid-particle mixture

$$\nabla.\vec{u} = 0 \quad \text{and} \quad \frac{d\rho\vec{u}}{dt} + \nabla.(\rho\vec{u}\otimes\vec{u}) = \nabla.\overline{\overline{\sigma}} + \rho\vec{g}$$

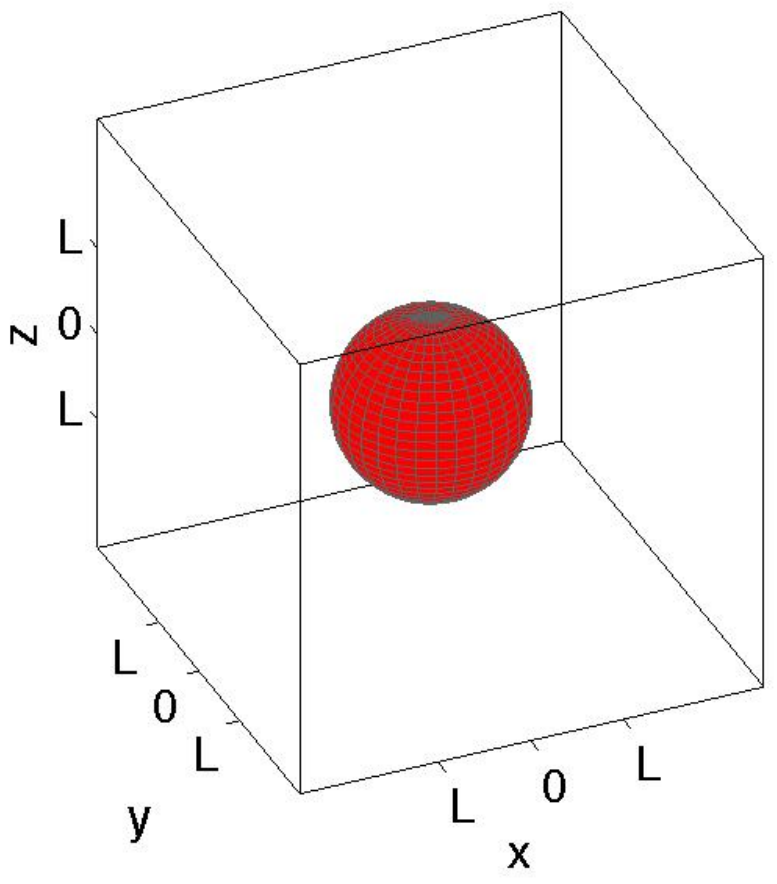

G_L is a 3D door function

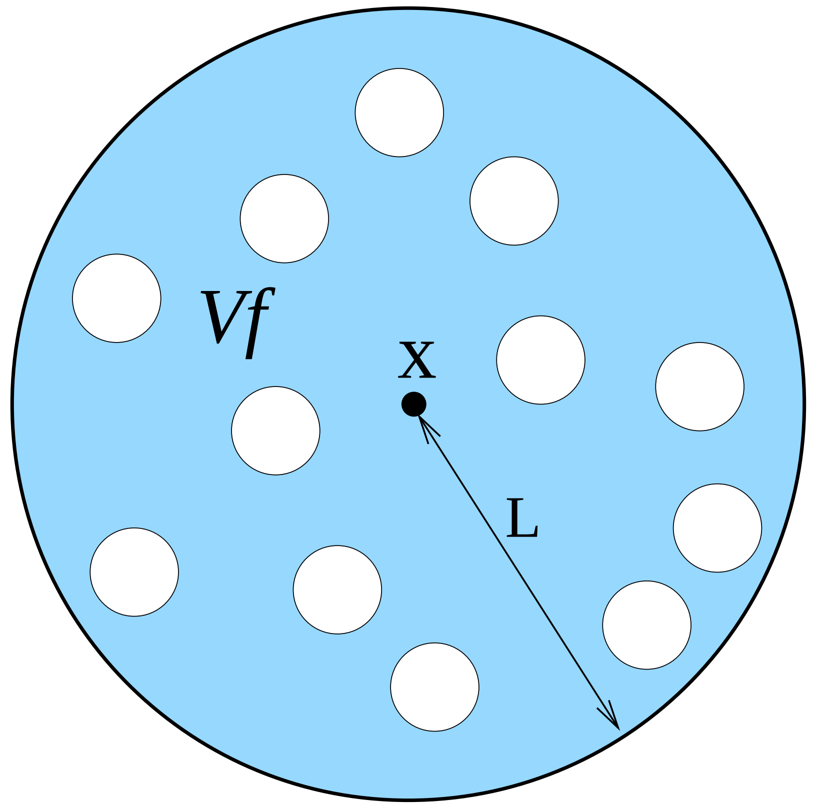

Local spatial averaging

Jackson (2000)

$$L_{flow} >> L >> d$$

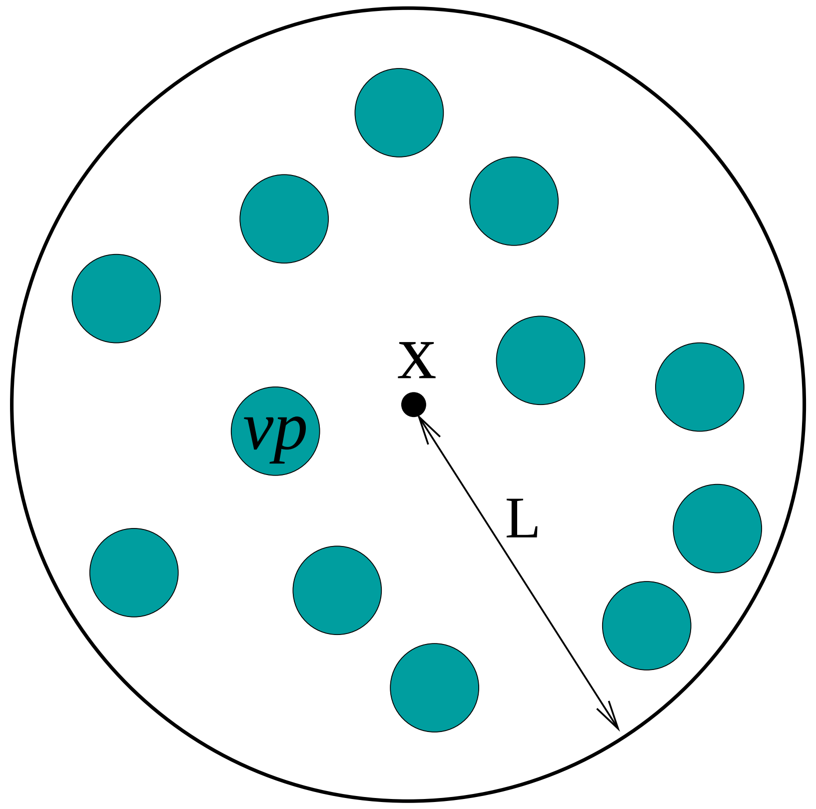

$$\langle f\rangle^f(\vec{x},t) = \frac{1}{1-\phi(\vec{x},t)}\int_{V_f(t)} f(\vec{y},t)G_L(|\vec{x}-\vec{y}|)dV_y$$

$$\langle f\rangle^p(\vec{x},t) = \frac{1}{\phi(\vec{x},t)}\sum_p \int_{v_p} f(\vec{y},t)G_L(|\vec{x}-\vec{y}|)dv_y$$

Fluid phase mass and momentum equations

$$\frac{\partial(1-\phi)}{\partial t} + \nabla\cdot\left((1-\phi)\langle\vec{u}\rangle^f\right) = 0$$

$$\rho^f\left[\frac{\partial(1-\phi)\langle\vec{u}\rangle^f}{\partial t} + \nabla\left((1-\phi)\langle\vec{u}\rangle^f\otimes\langle\vec{u}\rangle^f\right)\right] = \nabla\overline{\overline{\sigma}}^f - n\vec{f} + (1-\phi)\rho^f g$$

Eulerian-Eulerian two-phase flow equations

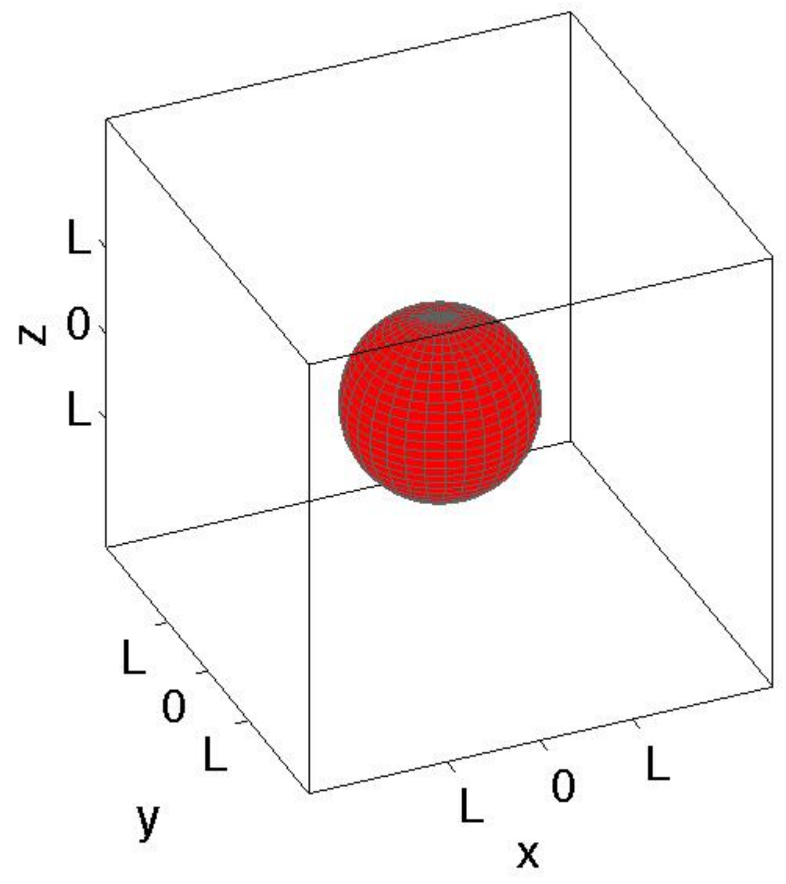

G_L is a 3D door function

Local mass & momentum conservation for a fluid-particle mixture

$$\nabla.\vec{u} = 0 \quad \text{and} \quad \frac{d\rho\vec{u}}{dt} + \nabla.(\rho\vec{u}\otimes\vec{u}) = \nabla.\overline{\overline{\sigma}} + \rho\vec{g}$$

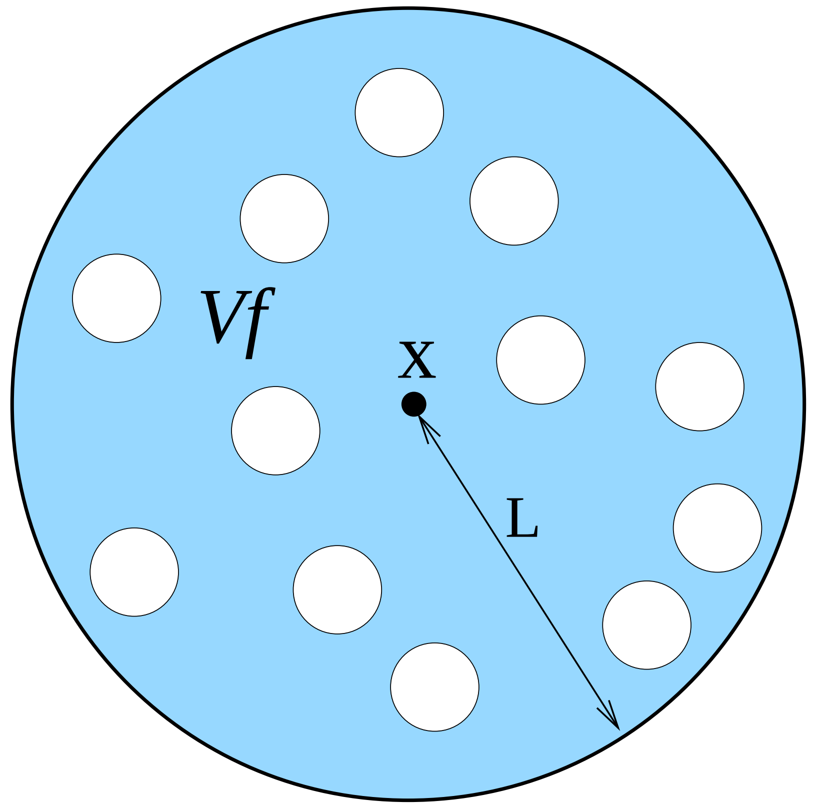

Local spatial averaging

Jackson (2000)

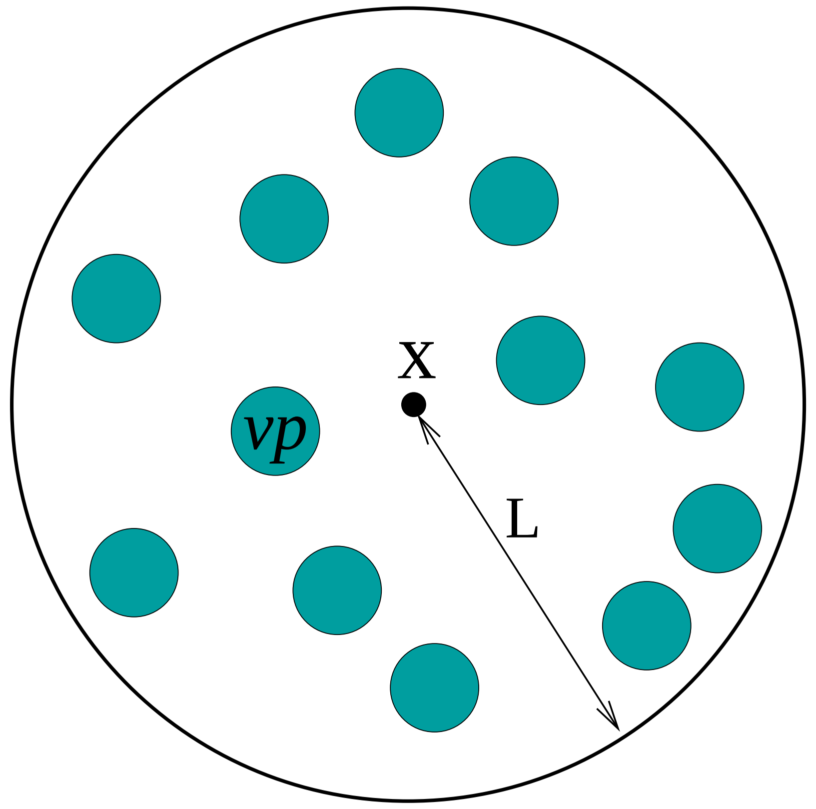

$$L_{flow} >> L >> d$$

$$\langle f\rangle^f(\vec{x},t) = \frac{1}{1-\phi(\vec{x},t)}\int_{V_f(t)} f(\vec{y},t)G_L(|\vec{x}-\vec{y}|)dV_y$$

$$\langle f\rangle^p(\vec{x},t) = \frac{1}{\phi(\vec{x},t)}\sum_p \int_{v_p} f(\vec{y},t)G_L(|\vec{x}-\vec{y}|)dv_y$$

Fluid phase mass and momentum equations

$$\frac{\partial(1-\phi)}{\partial t} + \nabla\cdot\left((1-\phi)\langle\vec{u}\rangle^f\right) = 0$$

$$\rho^f\left[\frac{\partial(1-\phi)\langle\vec{u}\rangle^f}{\partial t} + \nabla\left((1-\phi)\langle\vec{u}\rangle^f\otimes\langle\vec{u}\rangle^f\right)\right] = \nabla\overline{\overline{\sigma^f}} - n\vec{f} + (1-\phi)\rho^f g$$

Solid phase mass and momentum equations

$$\frac{\partial\phi}{\partial t} + \nabla\cdot\left(\phi\langle\vec{u}\rangle^p\right) = 0$$

$$\rho^p\left[\frac{\partial\phi\langle\vec{u}\rangle^p}{\partial t} + \nabla\left(\phi\langle\vec{u}\rangle^p\otimes\langle\vec{u}\rangle^p\right)\right] = \nabla\overline{\overline{\sigma^p}} + n\vec{f} + \phi\rho^p g$$

Favre-averaged two-phase flow equations

- Ensemble averaging: $\langle \phi \rangle = \lim_{N\to\infty} \sum_{k=1}^{N} \phi_k$ Favre-averaged velocity $\widetilde{\vec{u^f}}^f = \frac{\langle (1-\phi)\vec{u^f}\rangle}{1-\langle\phi\rangle}$ $\widetilde{\vec{u^p}}^p = \frac{\langle \phi\vec{u^p}\rangle}{\langle\phi\rangle}$
- Favre-averaged two-phase flow equations:

$$\frac{\partial\langle\epsilon\rangle}{\partial t} + \nabla\left(\langle\epsilon\rangle\,\widetilde{\vec{u^f}}^f\right) = 0$$

$$\rho^f\left[\frac{\partial\langle\epsilon\rangle\,\widetilde{\vec{u^f}}^f}{\partial t} + \nabla\left(\langle\epsilon\rangle\,\widetilde{\vec{u^f}}^f\otimes\widetilde{\vec{u^f}}^f\right)\right] = -\rho^f\nabla\left(\langle\epsilon\rangle\widetilde{\Delta u^f\otimes\Delta u^f}^f\right) - \vec{\nabla}p + \vec{\nabla}\cdot\overline{\overline{\tau^f}} - \langle n\vec{f}\rangle + \langle\epsilon\rangle\rho^f\vec{g}$$

$$\frac{\partial\langle\phi\rangle}{\partial t} + \nabla\left(\langle\phi\rangle\,\widetilde{\vec{u^p}}^p\right) = 0$$

$$\rho^p\left[\frac{\partial\langle\phi\rangle\,\widetilde{\vec{u^p}}^p}{\partial t} + \nabla\left(\langle\phi\rangle\,\widetilde{\vec{u^p}}^p\otimes\widetilde{\vec{u^p}}^p\right)\right] = -\rho^p\nabla\left(\langle\phi\rangle\widetilde{\Delta u^p\otimes\Delta u^p}^p\right) - \vec{\nabla}p^p + \vec{\nabla}\cdot\overline{\overline{\tau^p}} + \langle n\vec{f}\rangle + \langle\phi\rangle\rho^p\vec{g}$$

Effective fluid stress
Viscous effects ~ negligible

Reynolds-like stresses
Mixing length, k-ε or LES

Fluid-particle interactions
Drag + Buoyancy + dispersion

Granular stresses
μ(I) or Kinetic theory of granular flows

Two-fluid suspended-load simulation

Experiments with Glass Beads

Kiger & Pan (2002)

Parameters	Units	GB
U_b	$m.s^{-1}$	0.51
$u_\tau(\times 10^{-2})$	$m.s^{-1}$	2.99
h	m	0.02
ρ^s	$kg.m^{-3}$	2600
d_p	μm	195
$\phi_{tot}(\times 10^{-4})$	-	2.31
v_s/u_τ	-	0.87
Re_p	-	4.8
St	-	3.2
d_p/η	-	5.5

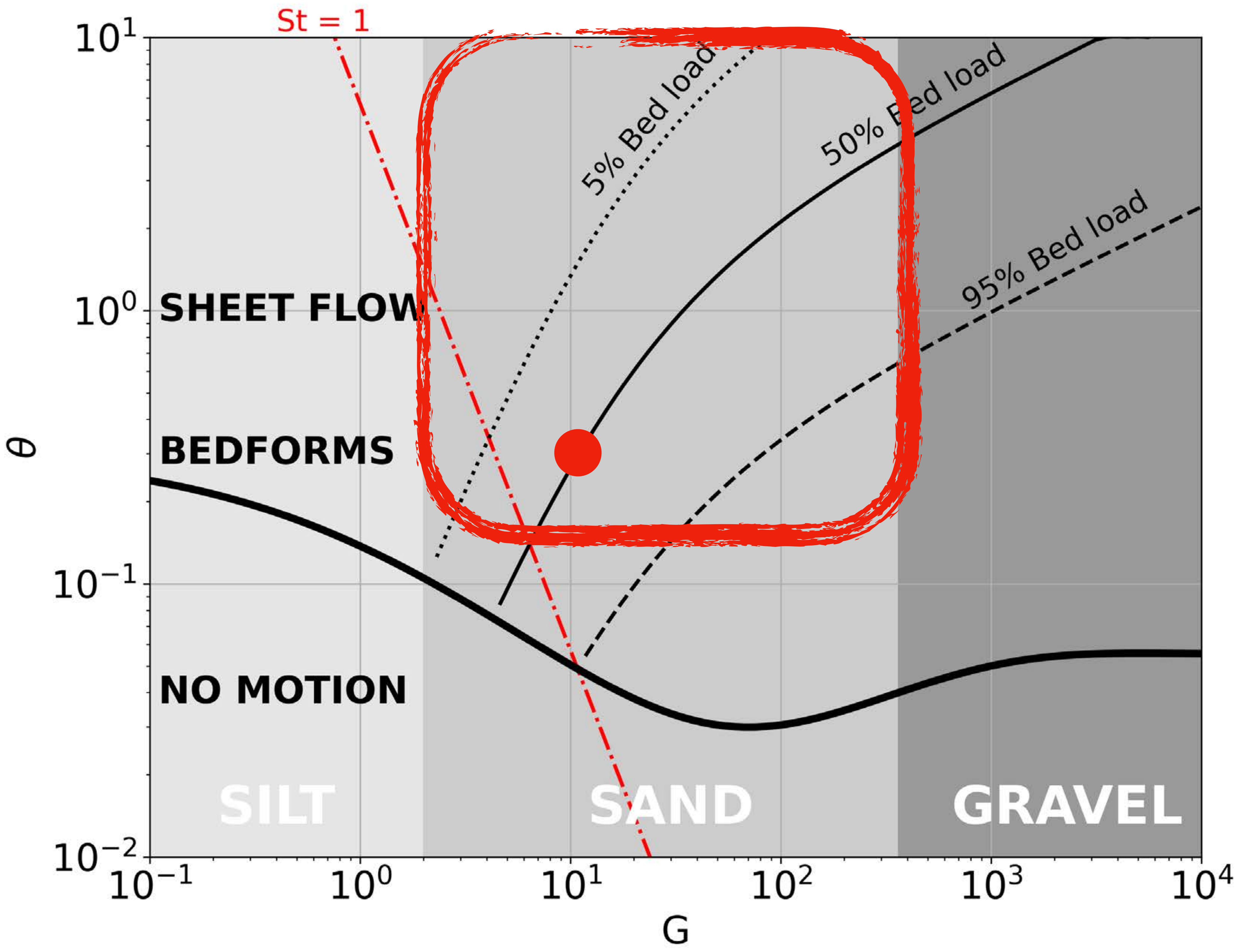

Two-fluid suspended-load simulation

Experiments with Glass Beads

Kiger & Pan (2002)

Parameters	Units	GB
U_b	$m.s^{-1}$	0.51
$u_\tau(\times 10^{-2})$	$m.s^{-1}$	2.99
h	m	0.02
ρ^s	$kg.m^{-3}$	2600
d_p	μm	195
$\phi_{tot}(\times 10^{-4})$	-	2.31
v_s/u_τ	-	0.87
Re_p	-	4.8
St	-	3.2
d_p/η	-	5.5

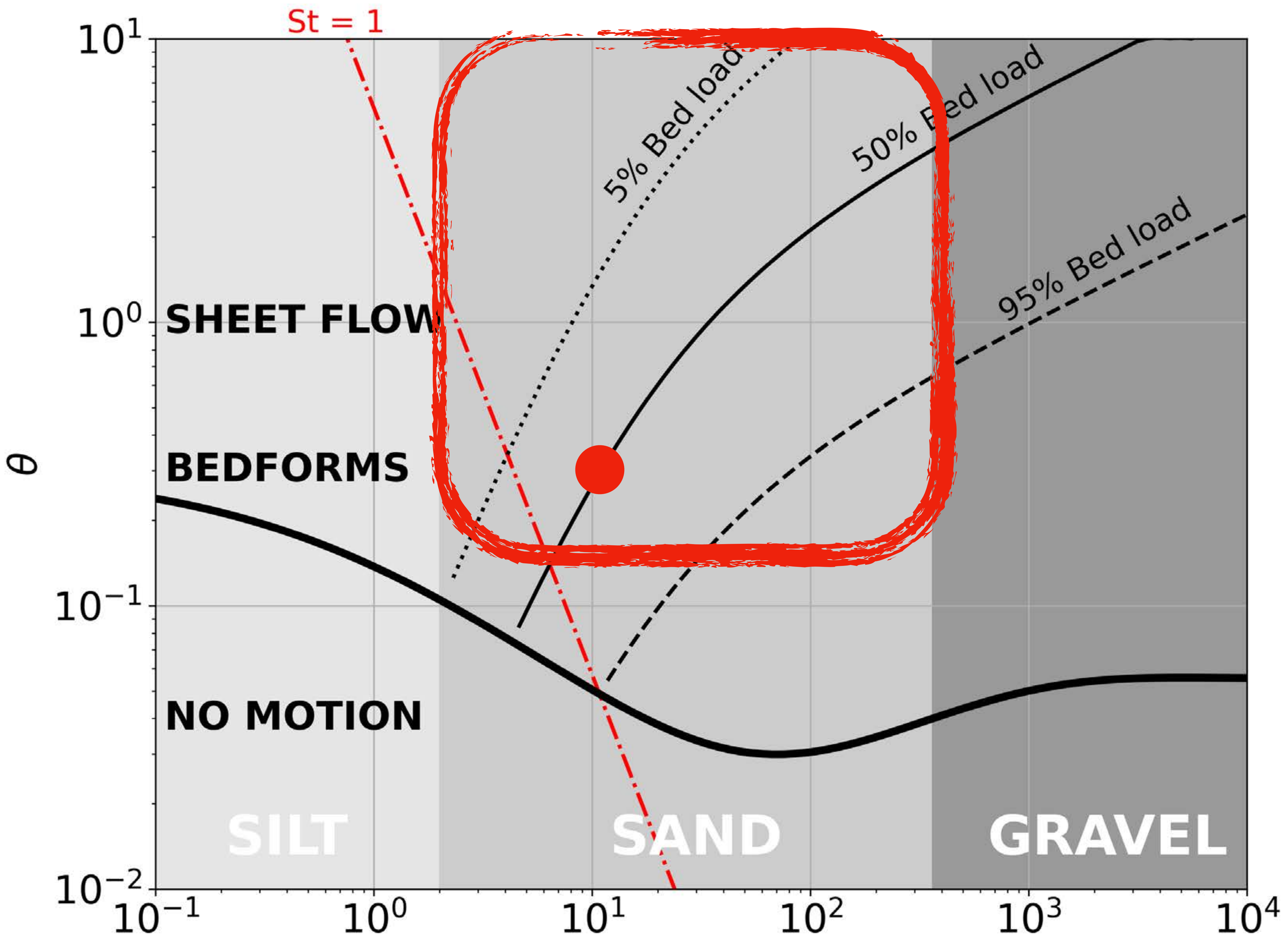

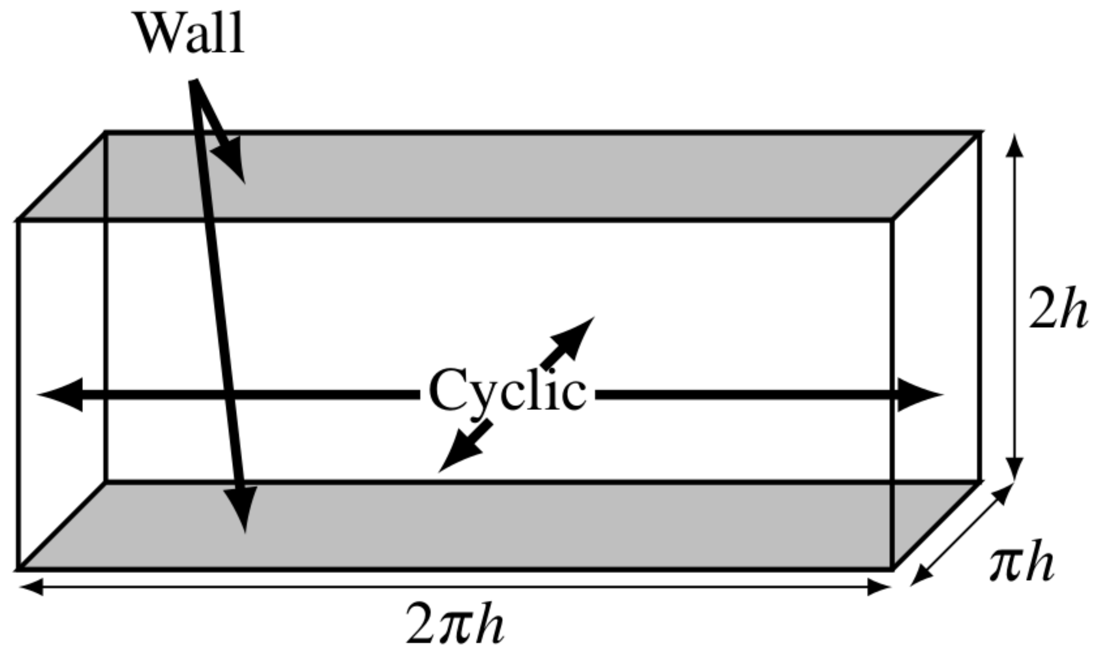

Numerical simulations: Mathieu et al. (JFM 2021)

- **2nd order finite volume** (openfoam/sedFOAM)
- **SGS model:** dynamic Lagrangian (Meneveau, 1996)

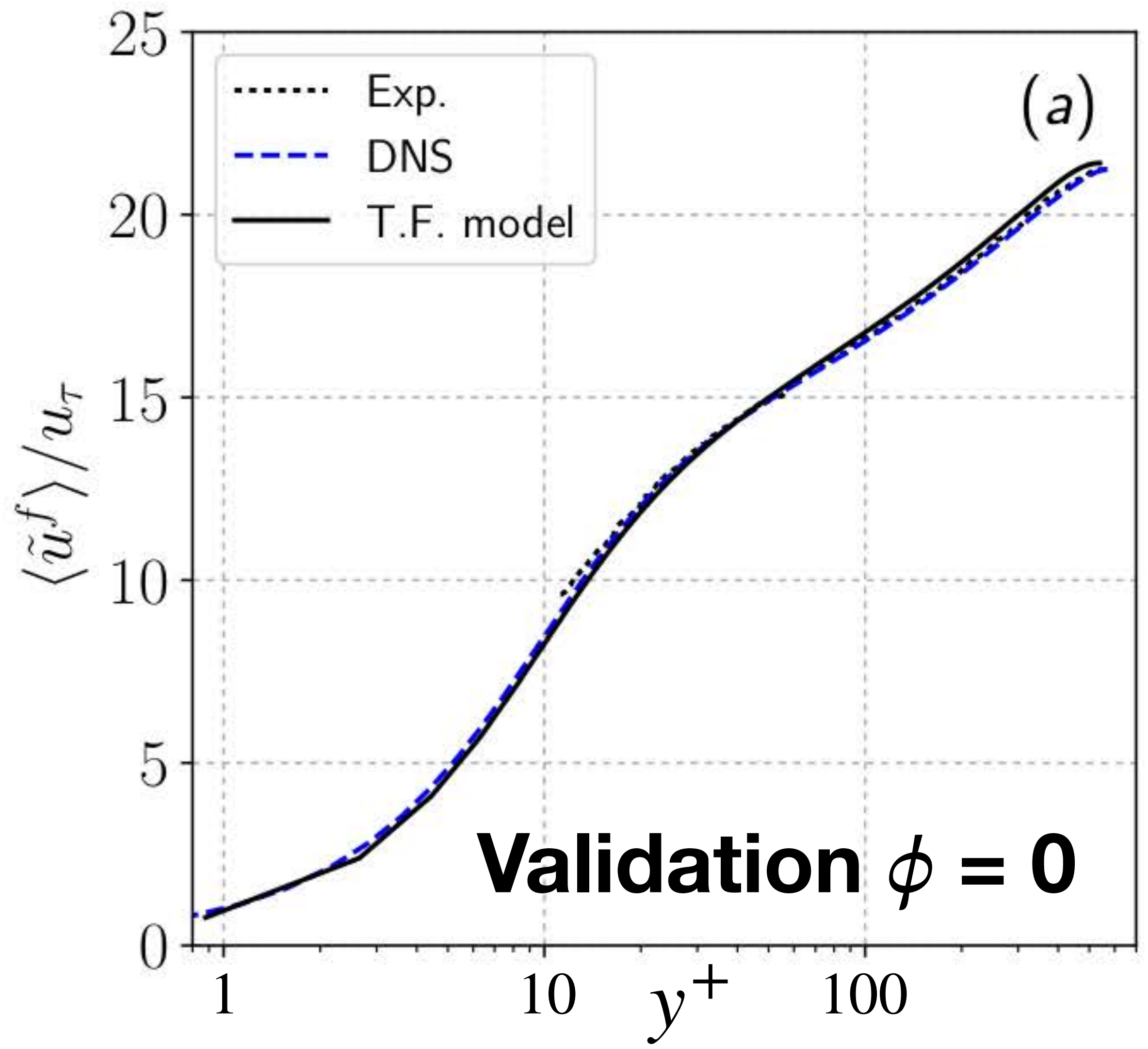

Mesh	Number of cells	Δ_x^+	Δ_z^+	Δ_y^+ (wall)
$314 \times 220 \times 160$	$11,105,280$	11	11	1

$$\frac{\Delta_x}{d_p} = \frac{\Delta_z}{d_p} \approx 2$$

Two-fluid suspended-load simulation

Glass beads experiments : Kiger & Pan (2002)

- $Re_b = 10^4$
- $Re_\tau = 560$
- $Re_p = 4.8$
- $St = 3.2$
- $d_p/\eta = 5.5$
- $\bar{\phi} = 2.31 \times 10^{-4}$

Contour of ϕ

Q criterion

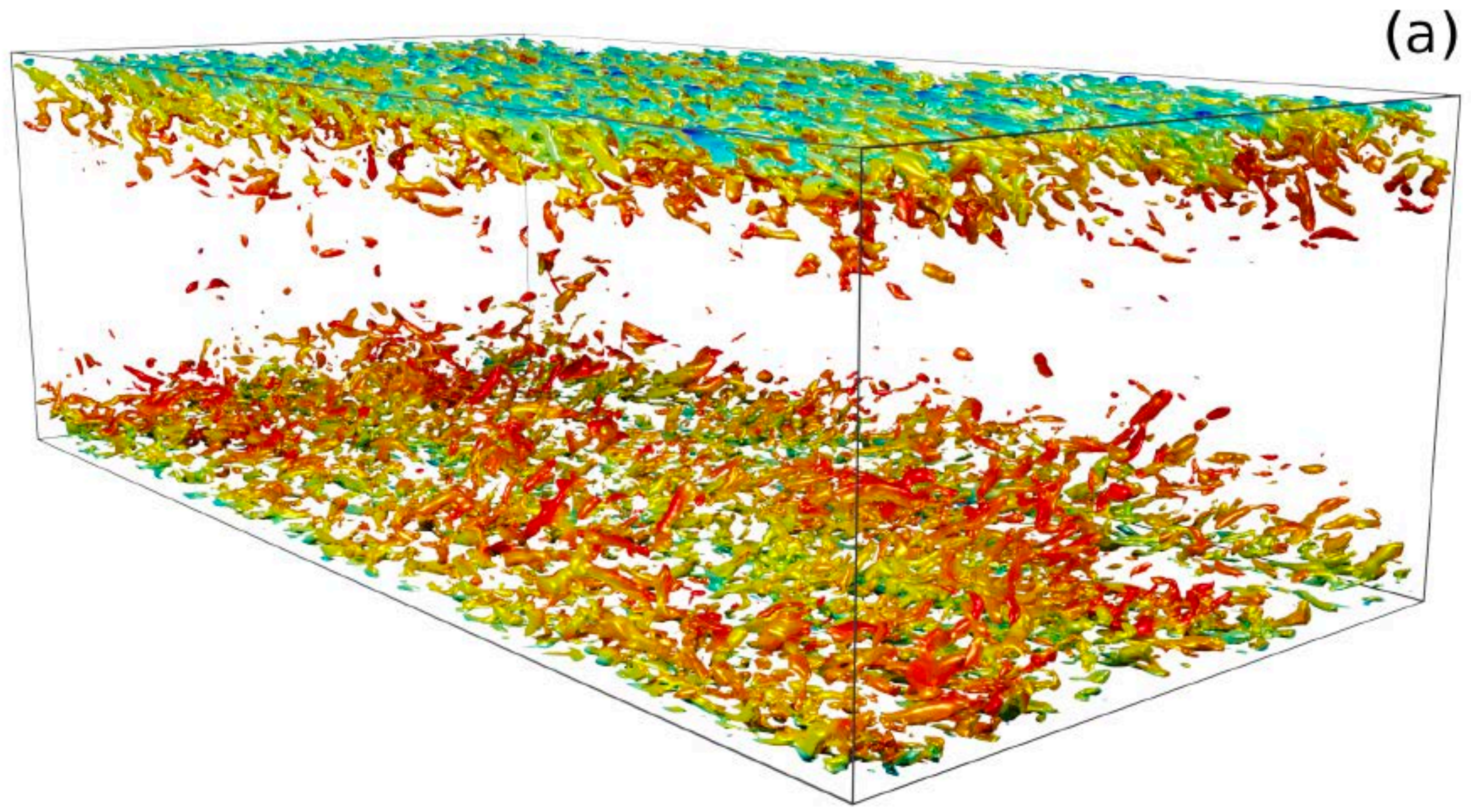

Mathieu et al. (JFM 2021)

Two-fluid suspended-load simulation

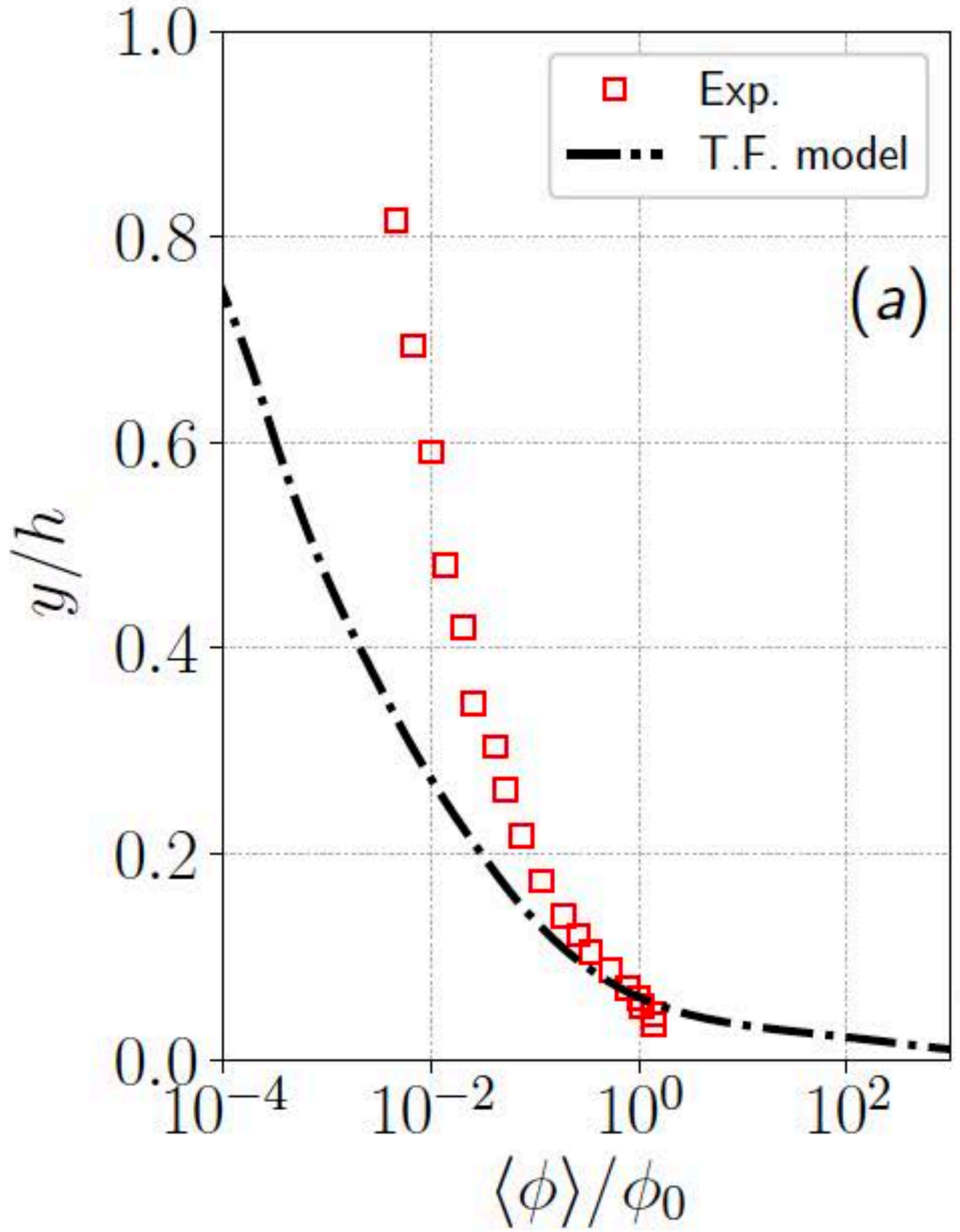

Glass beads experiments : Kiger & Pan (2002)

- $Re_b = 10^4$
- $Re_\tau = 560$
- $Re_p = 4.8$
- $St = 3.2$
- $d_p/\eta = 5.5$
- $\bar{\phi} = 2.31 \times 10^{-4}$

Contour of ϕ

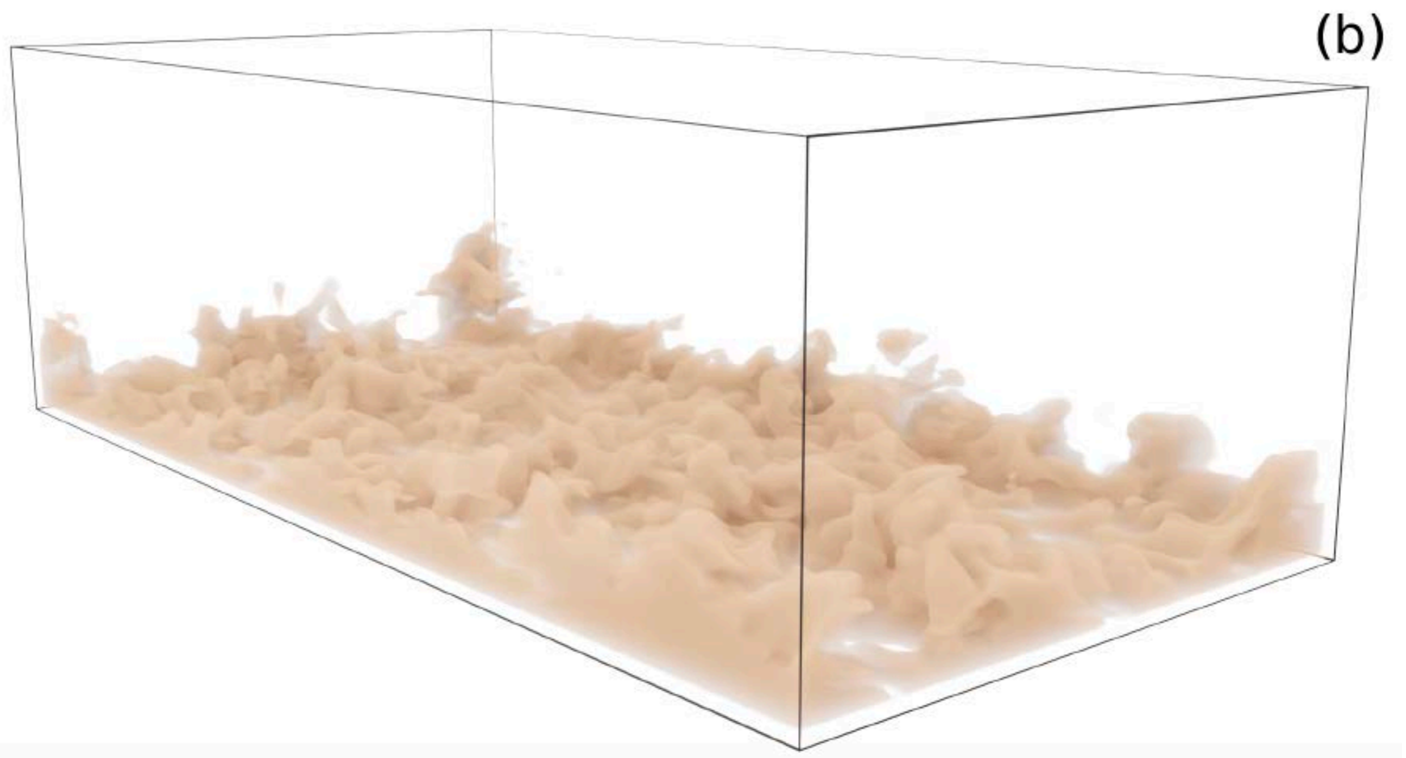

Q criterion

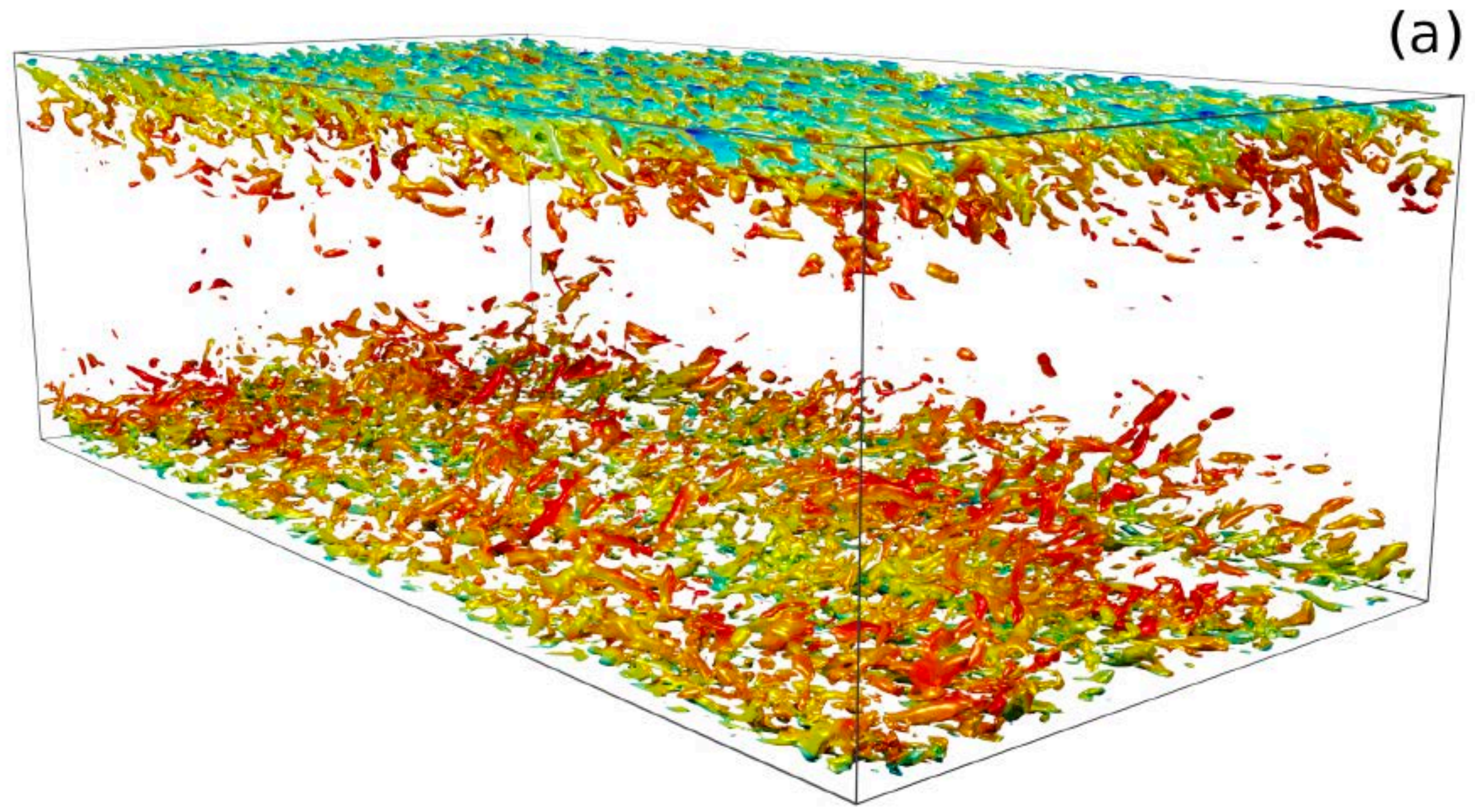

Mathieu et al. (JFM 2021)

Two-fluid suspended-load simulation

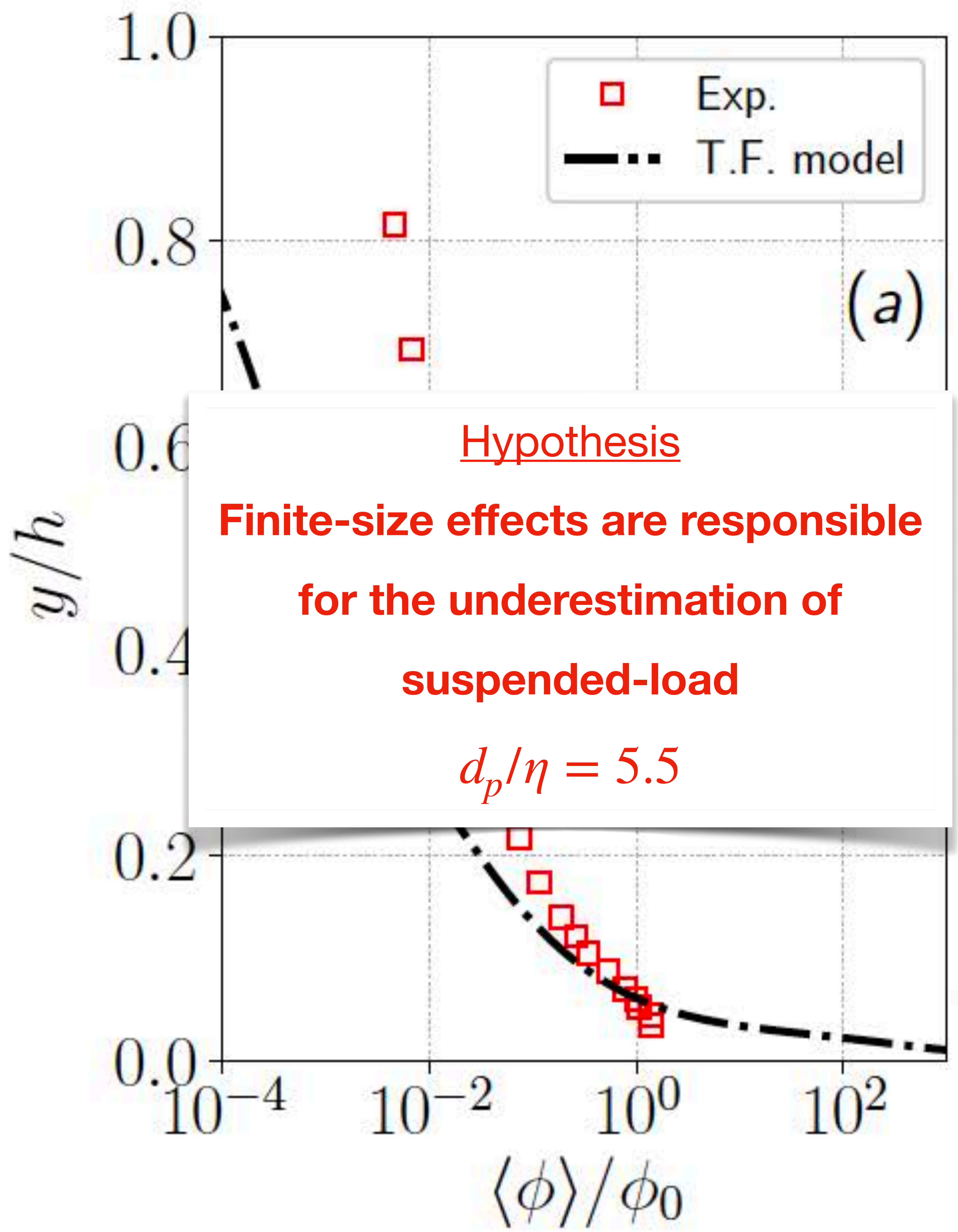

Hypothesis

Finite-size effects are responsible for the underestimation of suspended-load

$d_p/\eta = 5.5$

Glass beads experiments : Kiger & Pan (2002)

- $Re_b = 10^4$
- $Re_\tau = 560$
- $Re_p = 4.8$
- $St = 3.2$
- $d_p/\eta = 5.5$
- $\bar{\phi} = 2.31 \times 10^{-4}$

Contour of ϕ

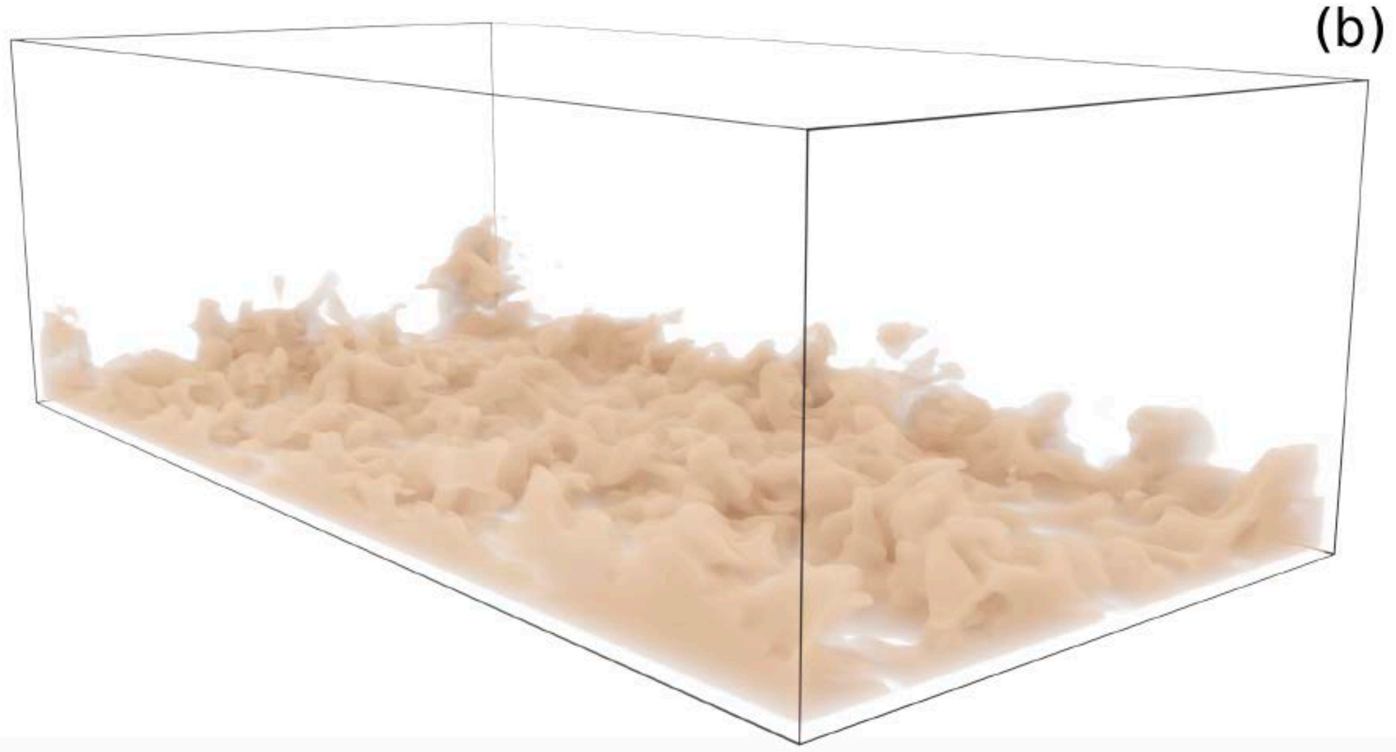

Q criterion

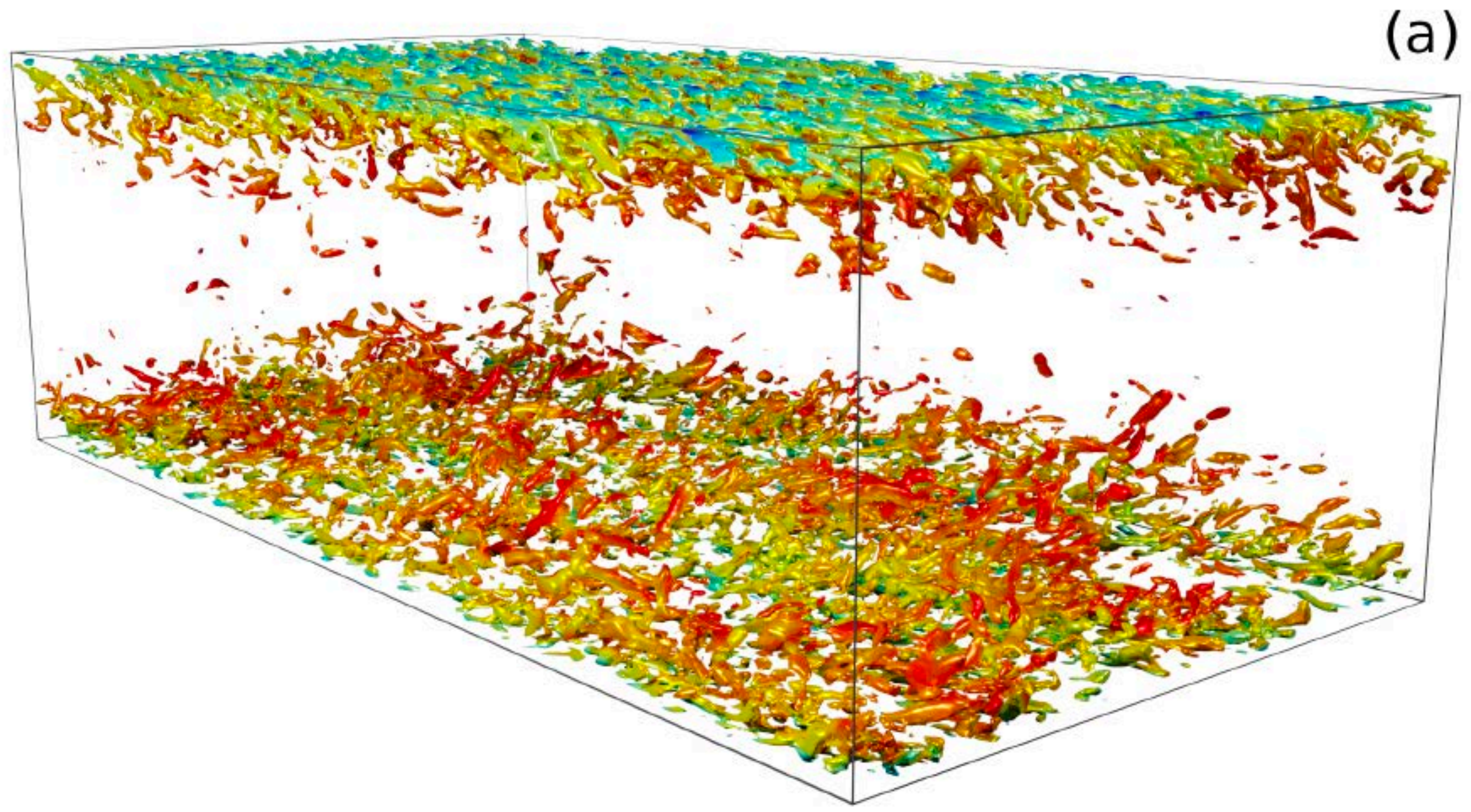

Mathieu et al. (JFM 2021)

Finite-size correction model for two-fluid LES

Finite-size particles

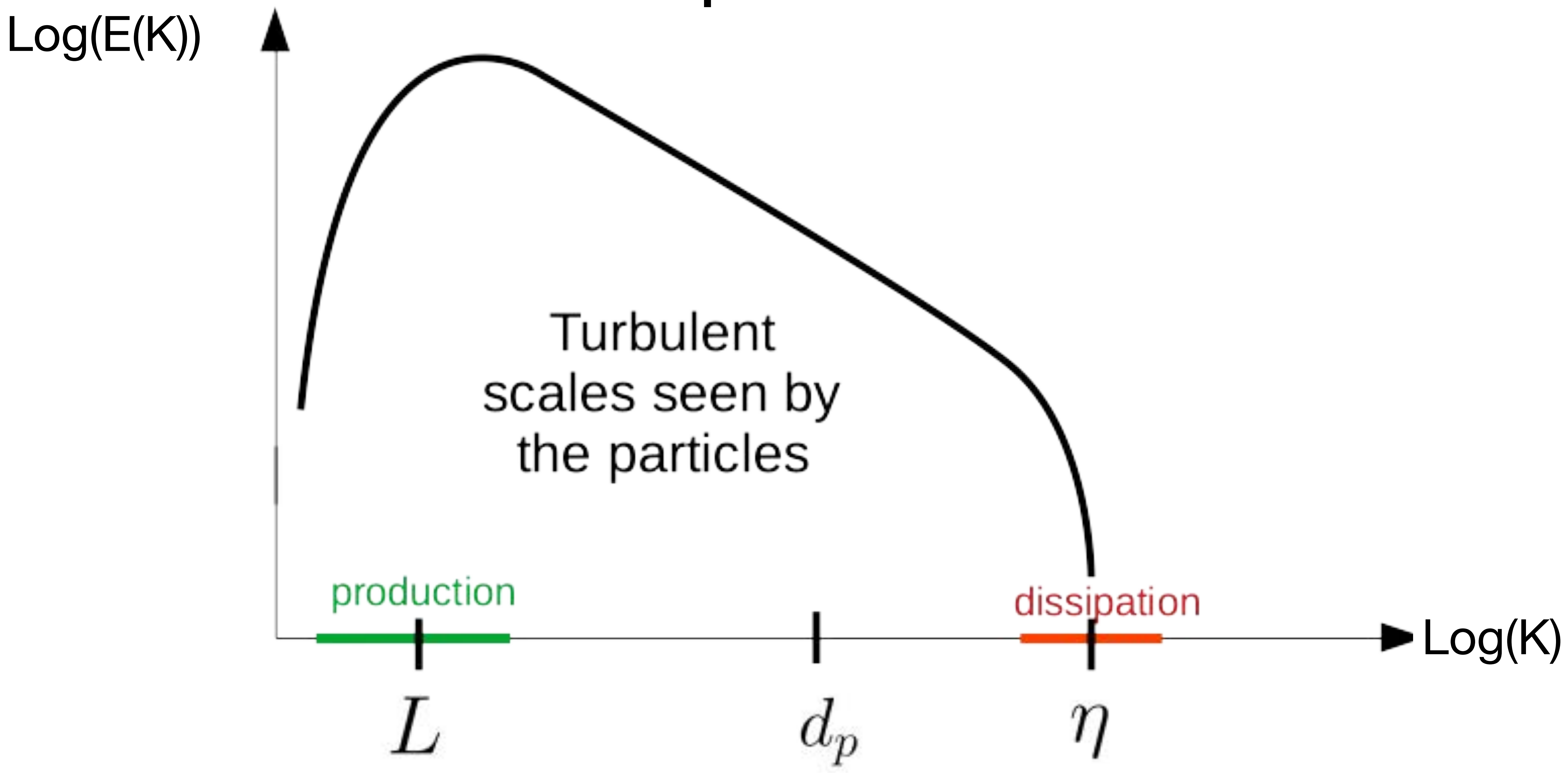

$L > d_p > \eta$

Mathieu et al. (JFM 2021)

Finite-size correction model for two-fluid LES

Finite-size particles

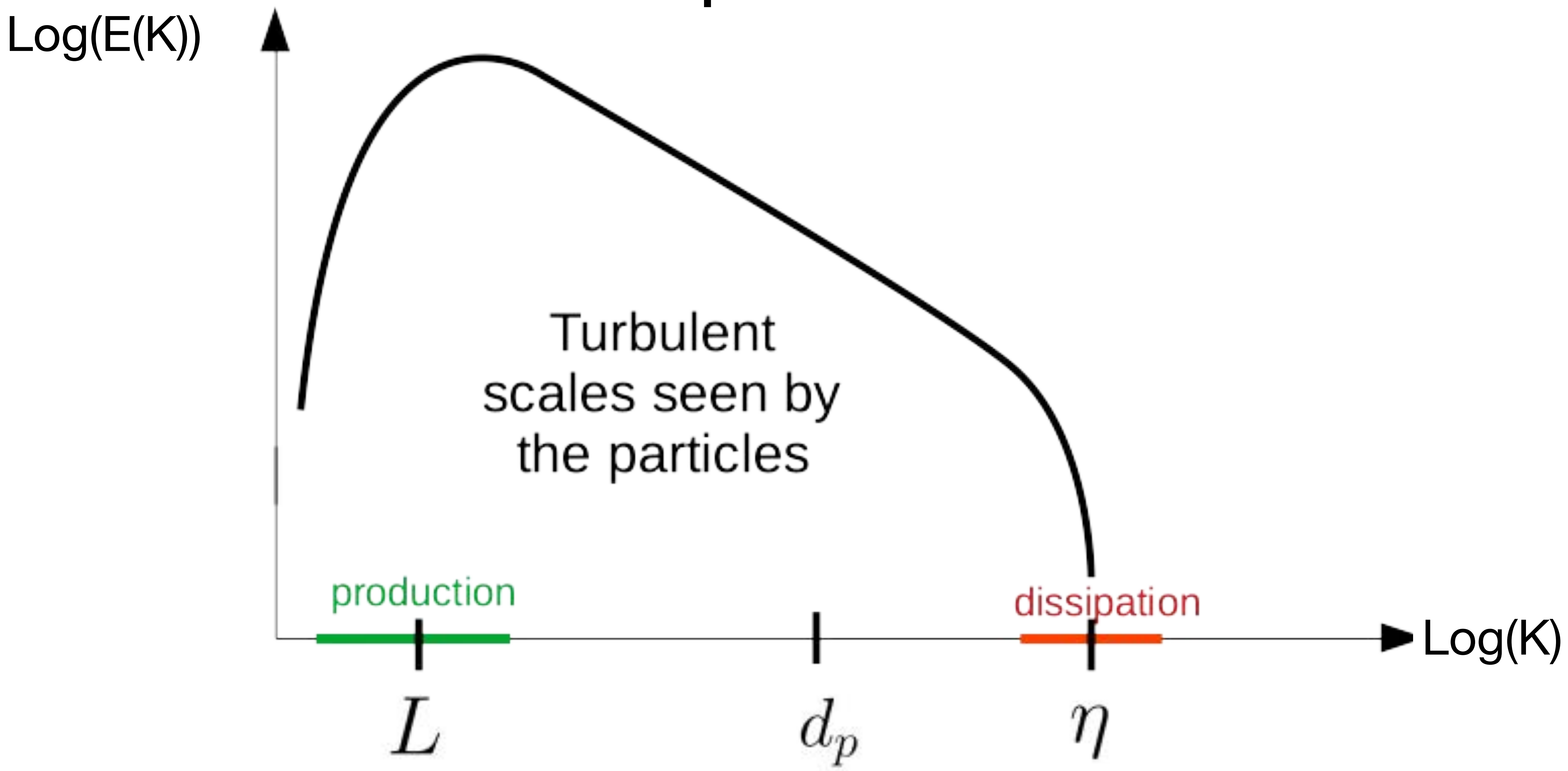

$$L > d_p > \eta$$

Spatial scales forcing the particles dynamics are filtered

➡ *Only turbulent structures larger than particle size do contribute to their advection*

Qureshi et al. (2007)

Mathieu et al. (JFM 2021)

Finite-size correction model for two-fluid LES

Finite-size particles

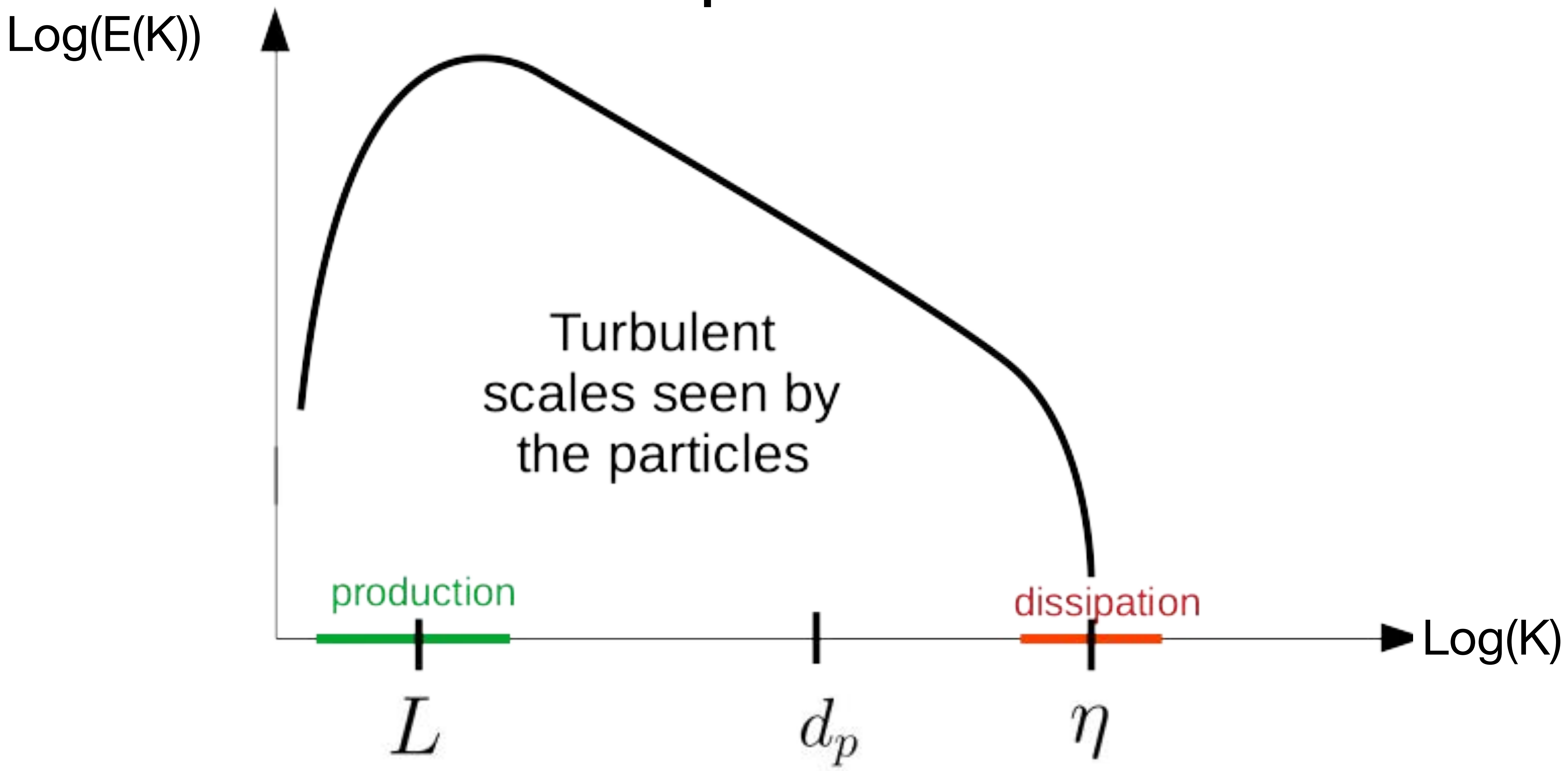

$L > d_p > \eta$

Drag force:

$$\bar{D}_i = \frac{\rho^s \bar{\phi}}{\tilde{t}_s} \left(\tilde{u}_i^f - \tilde{u}_i^s \right)$$

Particle relaxation time:

$$\tilde{t}_s = f\left(\|\tilde{u}_i^f - \tilde{u}_i^s\|,\ \nu^f \right)$$

Not valid anymore

Spatial scales forcing the particles dynamics are filtered

➡ *Only turbulent structures larger than particle size do contribute to their advection*

Qureshi et al. (2007)

Mathieu et al. (JFM 2021)

Finite-size correction model for two-fluid LES

Finite-size particles

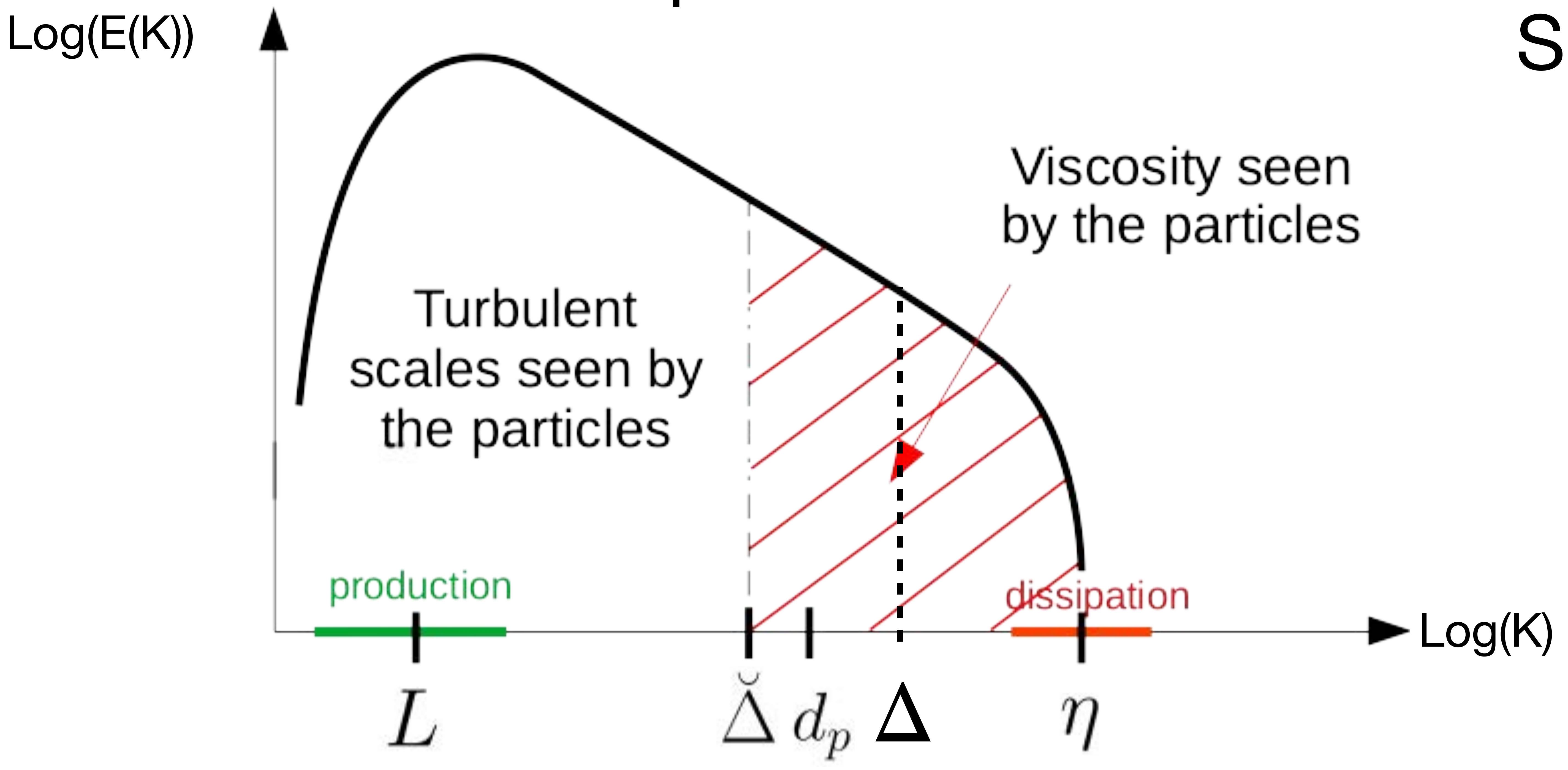

Spatial filter: $\breve{\Delta} = 2d_p$

Kidanemariam et al. (NJP 2013)

Eddies smaller than d_p modify the particle response time by increasing the viscosity "seen" by the particles

Gorokhovski & Zamansky (2018)

Mathieu et al. (JFM 2021)

Finite-size correction model for two-fluid LES

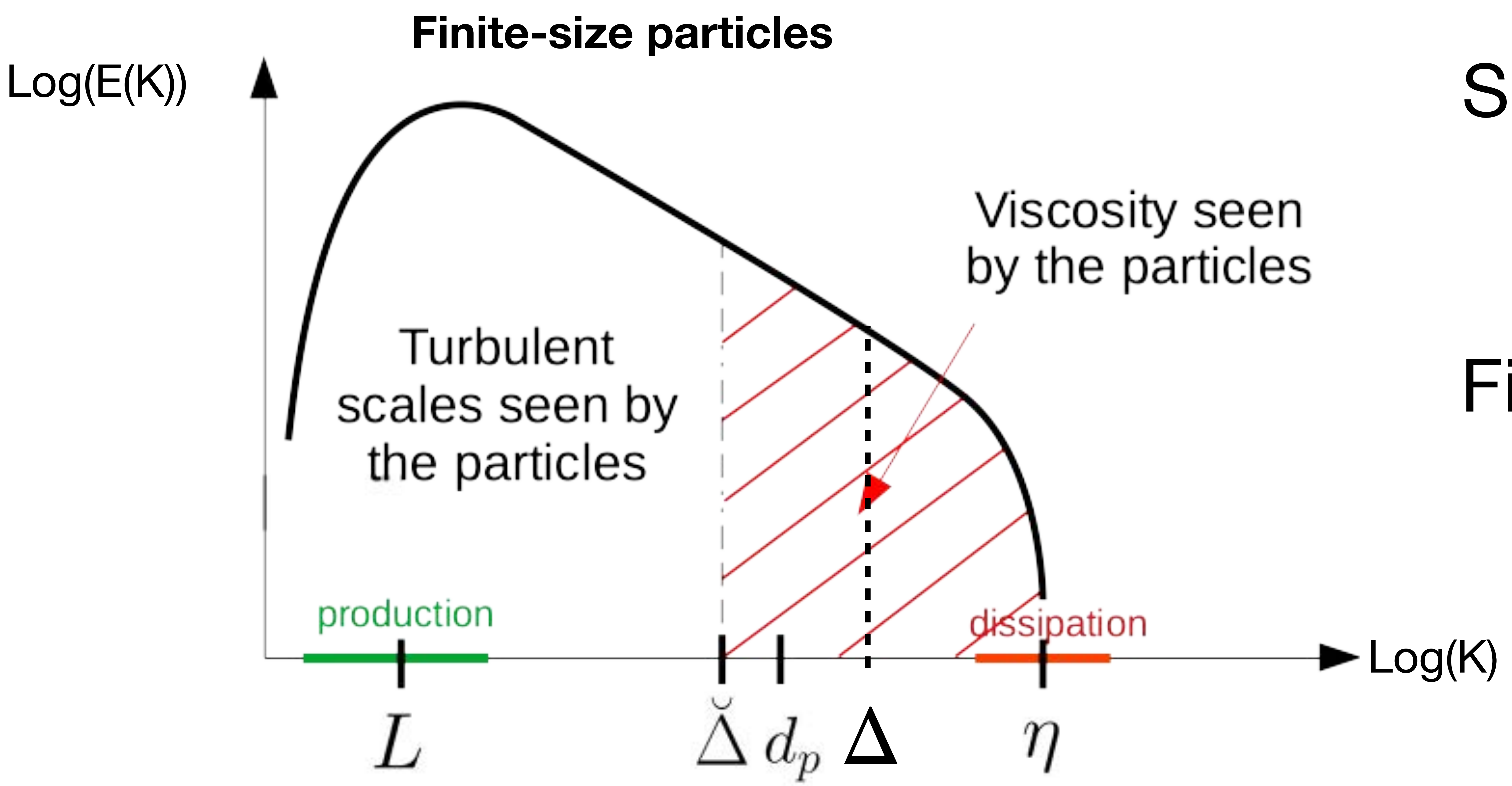

Eddies smaller than d_p modify the particle response time by increasing the viscosity "seen" by the particles

- Effective turbulent viscosity at the particle scale: $\nu_p^t \approx u_f' \, d_p \approx \varepsilon_p^{1/3} d_p^{4/3}$

Gorokhovski & Zamansky (2018)

Spatial filter: $\breve{\Delta} = 2d_p$

Kidanemariam et al. (NJP 2013)

Filtered drag force:

$$\bar{D}_i = \frac{\rho^s \bar{\phi}}{\tilde{t}_s} \left(\breve{u}_i^f - \tilde{u}_i^s \right)$$

Filtered particle relaxation time

$$\tilde{t}_s = f\left(\| \breve{u}_i^f - \tilde{u}_i^s \|, \; \nu^f + \nu_p^t \right)$$

Mathieu et al. (JFM 2021)

Finite-size correction model for two-fluid LES

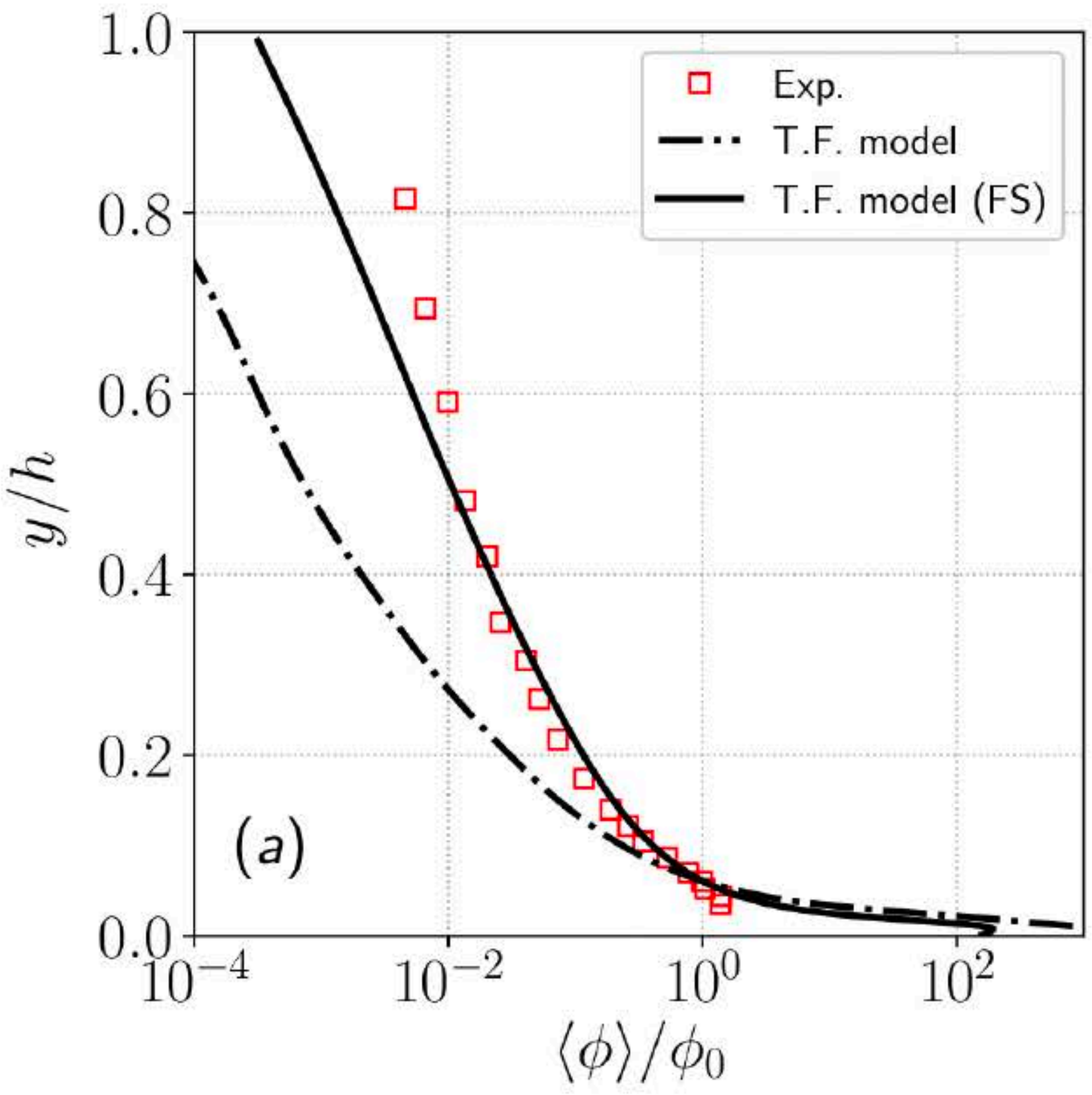

Eqn (5.10): $\dfrac{c}{c_r} = \left(\dfrac{z_r}{z}\right)^{R_o}$ with Prandtl mixing length: $\epsilon_s = \kappa\ u_*\ z$ and $R_o = \dfrac{w_s}{\kappa\ u_*}$ the Rouse number

Mathieu et al. (JFM 2021)

Finite-size correction model for two-fluid LES

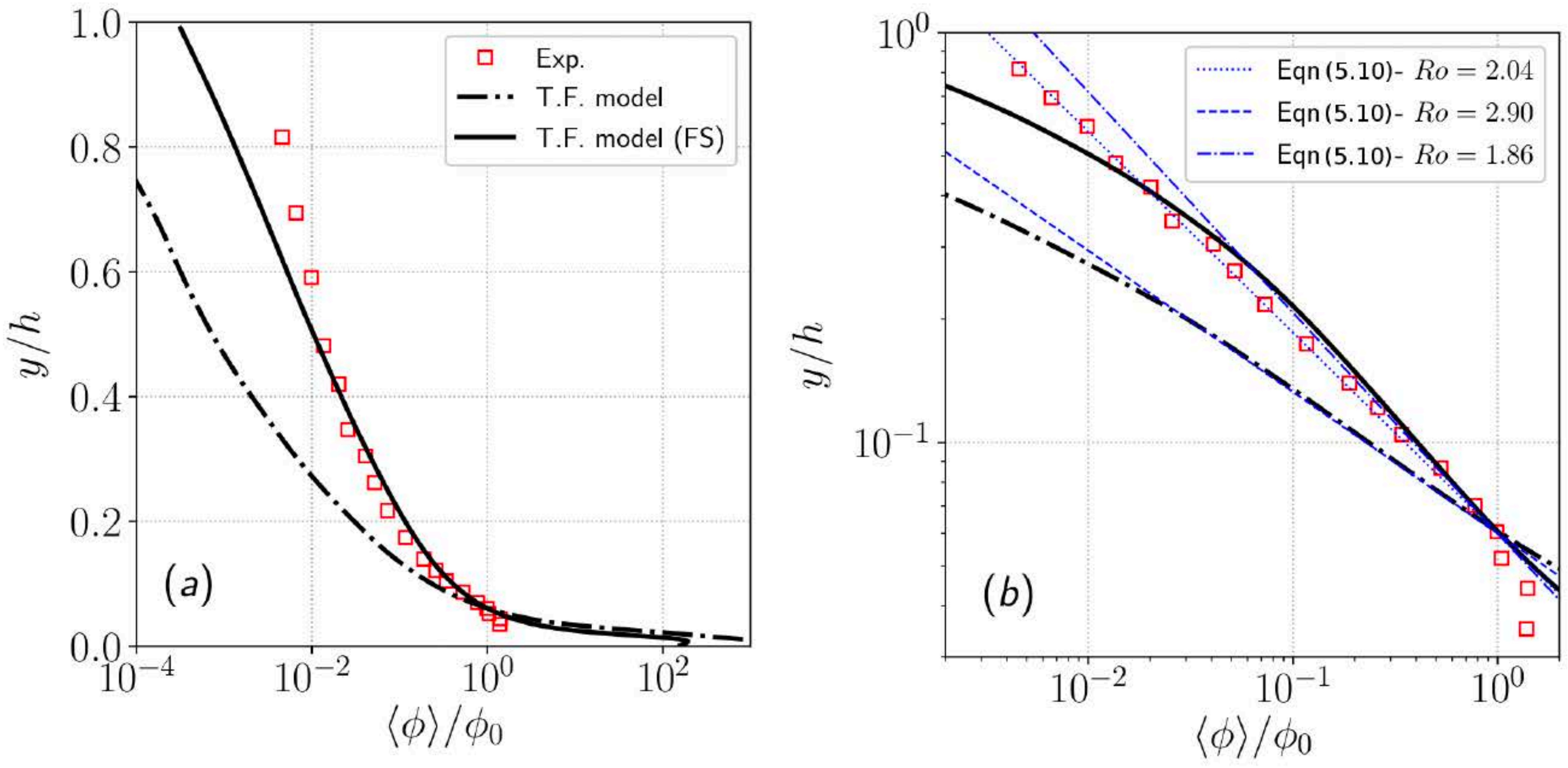

Eqn (5.10): $\frac{c}{c_r} = \left(\frac{z_r}{z}\right)^{R_o}$ with Prandtl mixing length: $\epsilon_s = \kappa\ u_*\ z$ and $R_o = \frac{w_s}{\kappa\ u_*}$ the Rouse number

Mathieu et al. (JFM 2021)

Finite-size correction model for two-fluid LES

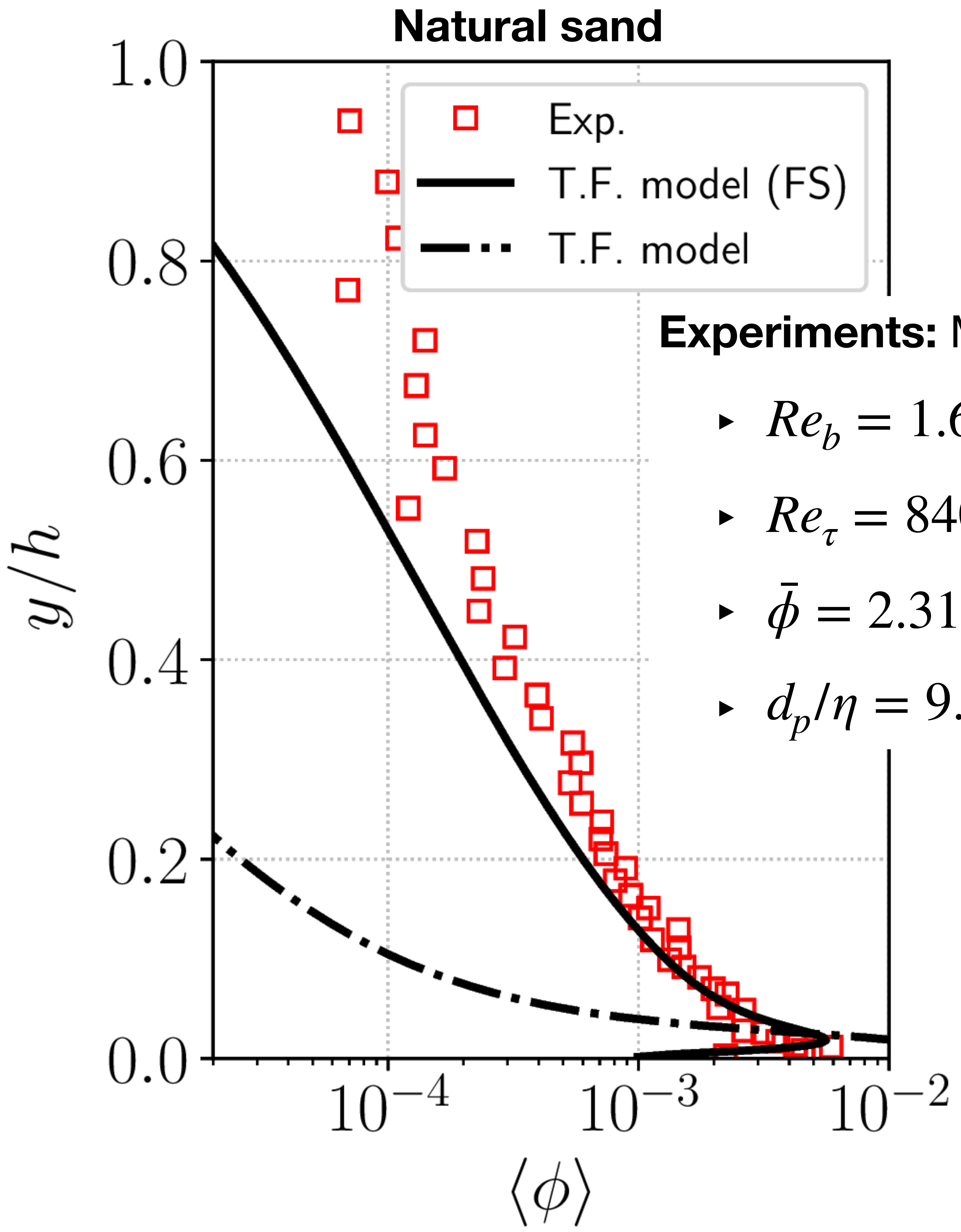

Experiments: Muste et al. (2005)

- $Re_b = 1.6 \times 10^4$
- $Re_\tau = 840$
- $\bar{\phi} = 2.31 \times 10^{-4}$
- $d_p/\eta = 9.7$

Mathieu et al. (JFM 2021)

Finite-size correction model for two-fluid LES

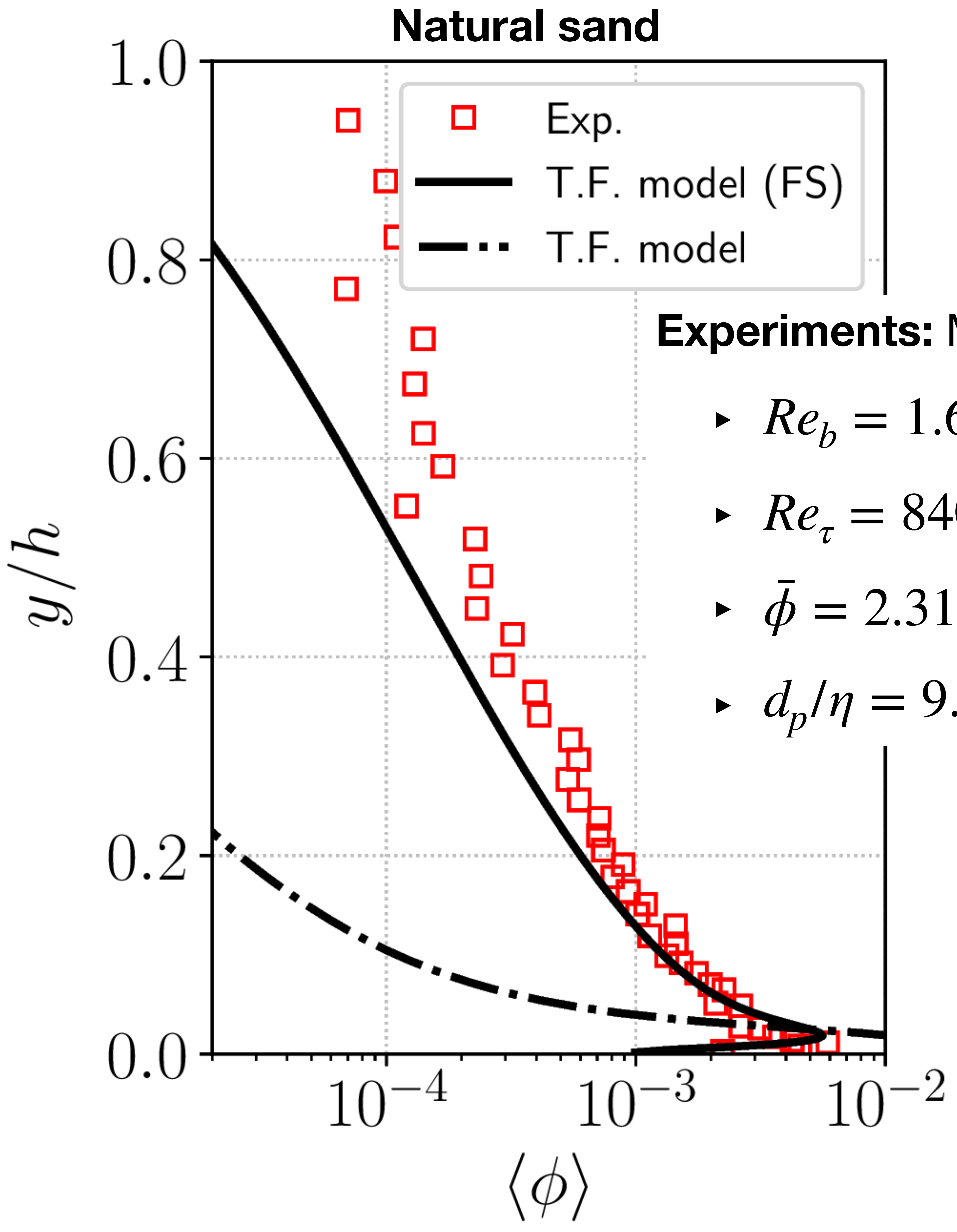

Experiments: Muste et al. (2005)

- $Re_b = 1.6 \times 10^4$
- $Re_\tau = 840$
- $\bar{\phi} = 2.31 \times 10^{-4}$
- $d_p/\eta = 9.7$

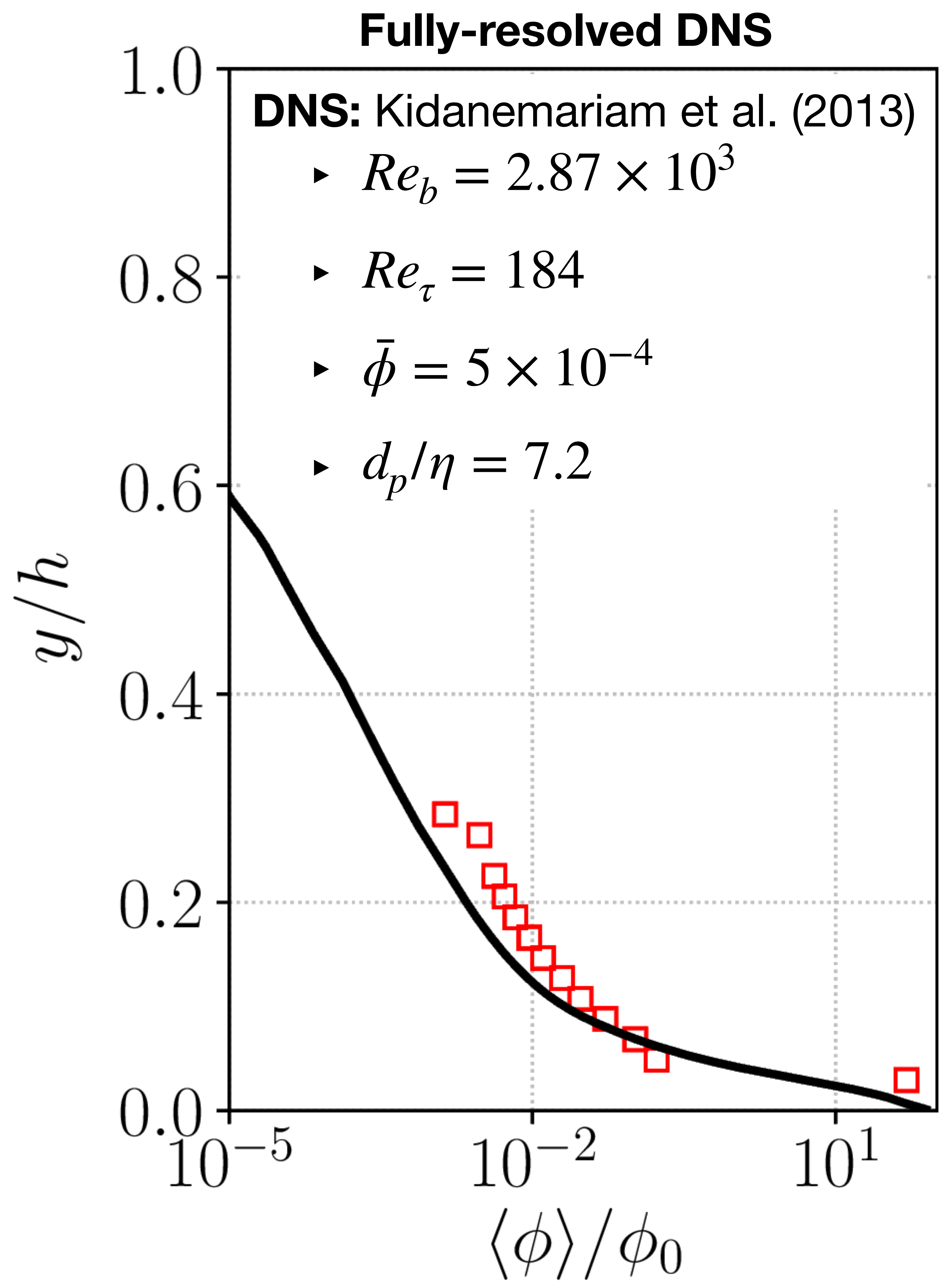

DNS: Kidanemariam et al. (2013)

- $Re_b = 2.87 \times 10^3$
- $Re_\tau = 184$
- $\bar{\phi} = 5 \times 10^{-4}$
- $d_p/\eta = 7.2$

Mathieu et al. (JFM 2021)

Finite-size correction model for two-fluid LES

Natural sand

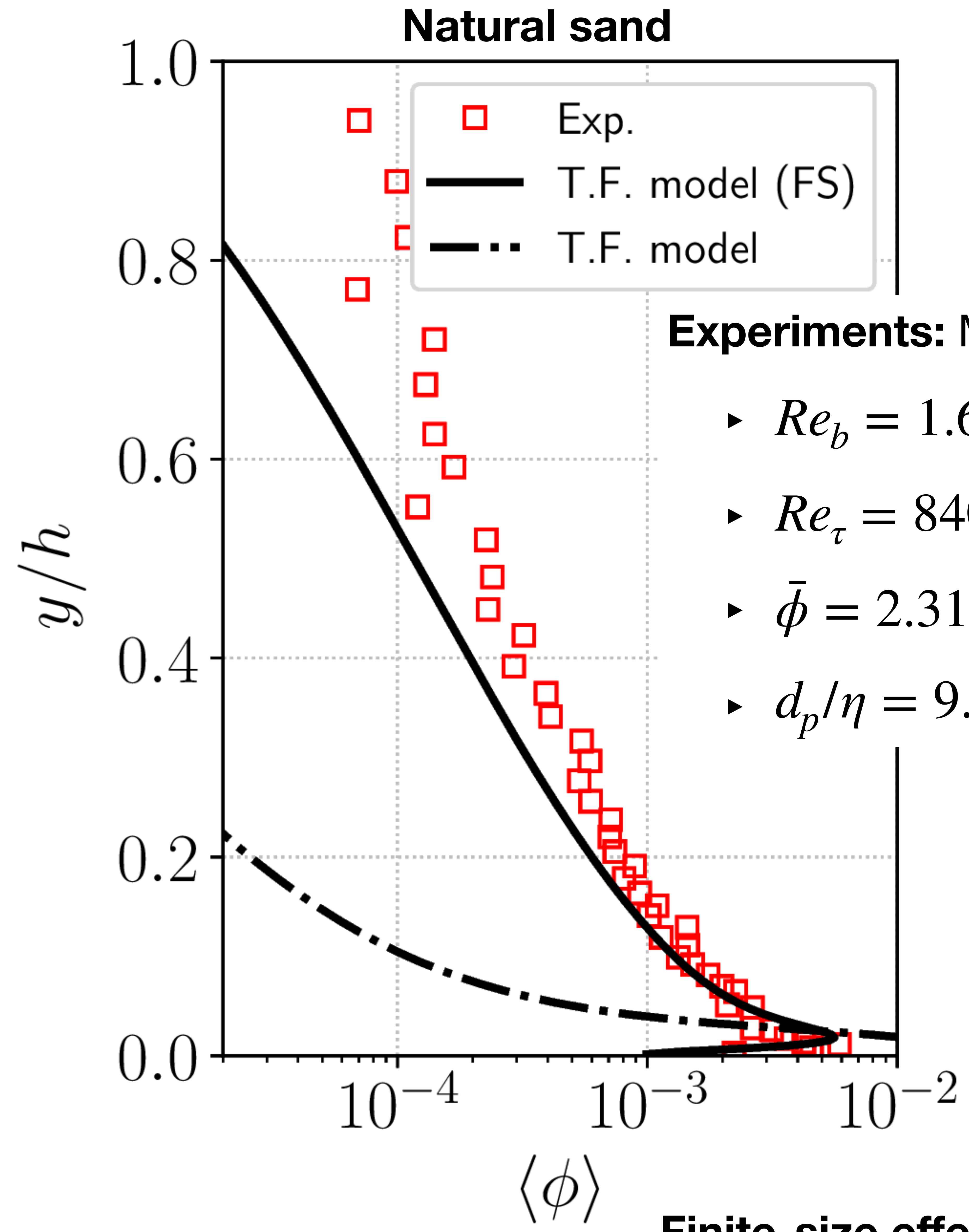

Experiments: Muste et al. (2005)

- $Re_b = 1.6 \times 10^4$
- $Re_\tau = 840$
- $\bar{\phi} = 2.31 \times 10^{-4}$
- $d_p/\eta = 9.7$

Fully-resolved DNS

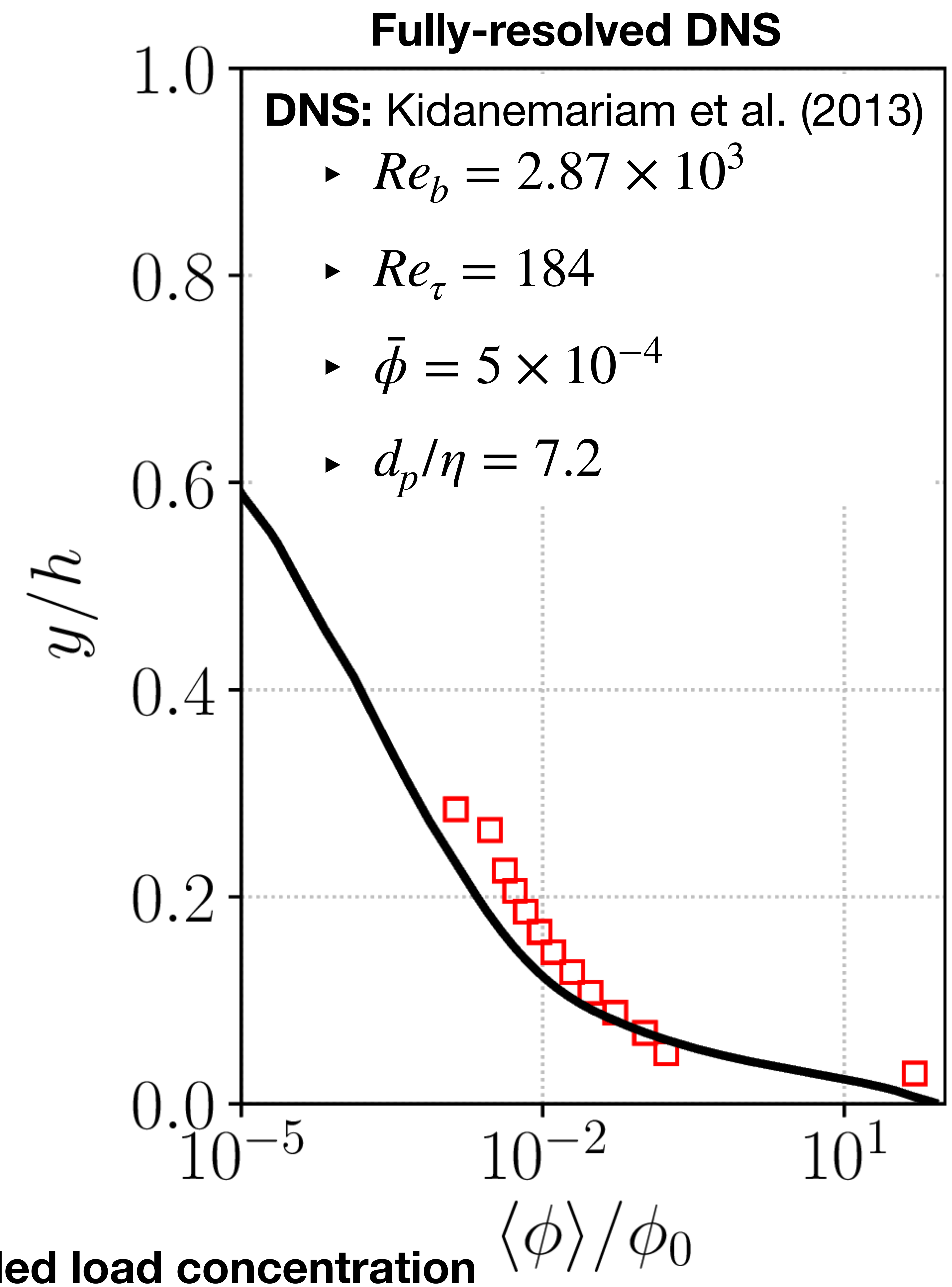

Finite-size effects increase suspended load concentration

Mathieu et al. (JFM 2021)

WHAT COULD EXPLAIN $S_c < 1$?

Sediment mass balance: $$W_s \langle \phi \rangle + \frac{\nu^t}{S_c} \frac{d \langle \phi \rangle}{dy} = 0$$

WHAT COULD EXPLAIN $S_c < 1$?

Sediment mass balance: $$W_s\langle\phi\rangle + \frac{\nu^t}{S_c}\frac{d\langle\phi\rangle}{dy} = 0$$

$$S_c < 1 \Longleftrightarrow W_s \downarrow$$

WHAT COULD EXPLAIN $S_c < 1$?

Sediment mass balance: $$W_s\langle\phi\rangle + \frac{\nu^t}{S_c}\frac{d\langle\phi\rangle}{dy} = 0$$

$$S_c < 1 \iff W_s \downarrow$$

The turbulent Schmidt number is not smaller than unity

BUT

settling velocity is reduced due to finite-size effects

Other evidence of settling retardation are presented in Chauchat et al. (PRF 2022)

Conclusions

Finite size effects on suspended-load

➡ They are significant for medium sand particles

➡ They can be modeled using a sub grid scale viscosity in the drag force

➡ They might explain why the turbulent Schmidt number has been taken as Sc < 1

Perspectives

➡ Extent the approach to larger size ratios: $d_p/\eta > 10$

➡ Apply the two-fluid LES to wave-driven sand transport and ripples formation

sedFOAM team

LEGI
Univ. Grenoble Alpes
France


C. Bonamy


E. Puig-Montella


R. Chassagne


A. Gilletta

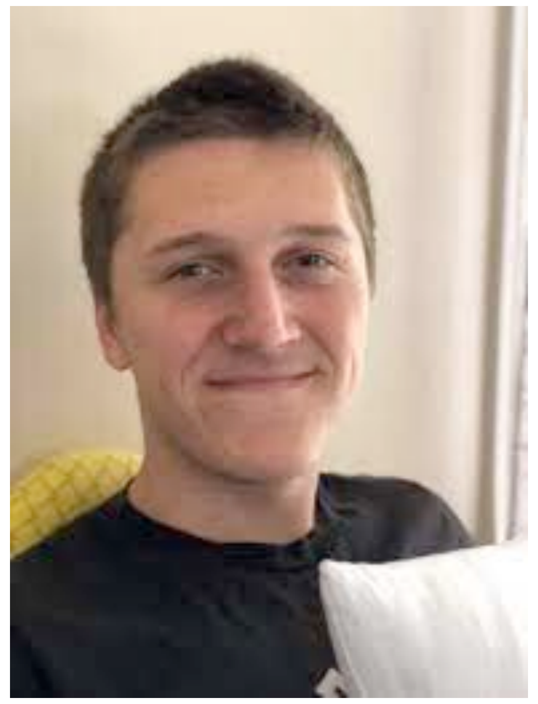
H. Divel

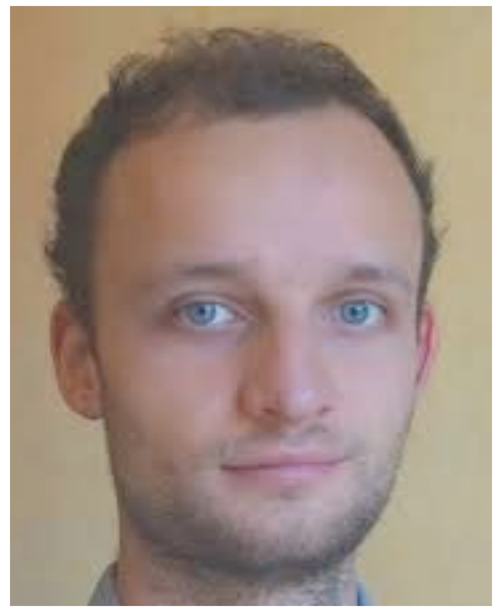
A. Mathieu


T. Nagel


T. Revil-Baudard

...

CACR
Univ. Delaware
USA


T.-J. Hsu.


Z. Cheng


A. Salimi Tarazouj

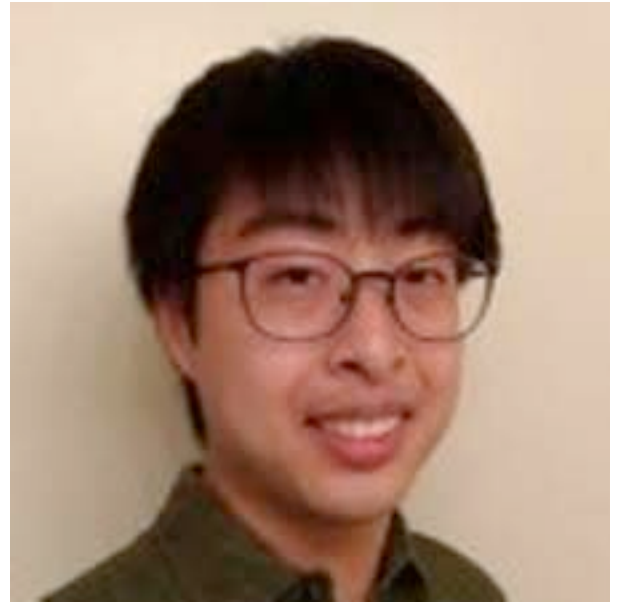
B. Tsai

...